SAND2007-2674P

INTERACTION FORCES MEASURED BY ATOMIC FORCE MICROSCOPY FOR MUSCOVITE AND CARBOXYL-MODIFIED MICROSPHERES AS A FUNCTION OF IONIC STRENGTH

by

Marissa D. Reno

April, 2007

Submitted in partial fulfillment of
the requirements for a Master of
Science Degree in Hydrology

New Mexico Institute of Mining and Technology
Socorro, New Mexico

ABSTRACT

This research used atomic force microscopy (AFM) to gain a better understanding of the interactions between muscovite mica and a model colloid used commonly throughout the existing colloid transport literature. The interaction forces between a single crystal muscovite mica disc and a 2.0-μm carboxyl-modified polystyrene latex microsphere attached to a tipless silicon nitride (SiN) cantilever were measured in KCl solutions of varying ionic strength (10, 30, 100, and 300 mM) using AFM. The three main objectives of this work were to 1) directly measure the interaction forces between muscovite mica and carboxyl-modified polystyrene latex microspheres, 2) evaluate the magnitude and significance of surface charge heterogeneities on the muscovite surface by making AFM measurements at multiple spatial locations, and 3) evaluate the feasibility of measuring the secondary energy minimum using conventional AFM instrumentation. AFM measurements were shown to be qualitatively reproducible only when strict surface preparation techniques were employed and a well-developed experimental protocol was adhered to. For measurements taken at various ionic strengths, repulsive forces were observed to decrease at higher ionic strengths. The tip-sample separation distance at which repulsive forces were first observed increased at lower ionic strengths. Both of these observations are in accord with theoretical predictions of Derjaguin-Landau-

Verwey-Overbeek (DLVO) theory. Measurements taken at several spatial locations on the muscovite surface suggested that there is heterogeneity in the muscovite surface properties. This heterogeneity was within the range of forces predicted by DLVO calculations using bounding values of ζ-potential and Hamaker constant. Variability in the tip-sample separation distance at the primary barrier was greater at a lower ionic strength than at a higher ionic strength for both AFM measurements and DLVO predictions. With the instrumentation used in this work, excessive noise and insufficient cantilever sensitivity made measurement of the secondary energy minimum infeasible. The results suggest that AFM is a useful tool for direct measurement of interaction forces and confirmation of theoretical predictions.

The major results outlined above are augmented by the content of several appendices. Background AFM information is given, including a useful description on interpretation of theoretically-calculated and measured interaction forces. The process by which numerical artifacts arose and were dealt with is detailed. Finally, force measurements conducted between a silica surface and a 2.0-μm carboxyl-modified polystyrene latex microsphere, not included in the major results, are described and commented on, including the reason for their exclusion. A data CD with all raw and manipulated data used for the figures and discussions in this work, in addition to an extensive reference list, are provided to facilitate the use of this thesis project as a reference tool for future researchers.

ACKNOWLEDGEMENTS

I would like to thank Sandia National Laboratories' Laboratory Directed Research and Development (LDRD) program and the Department of Energy, Office of Civilian Radioactive Waste Management (OCRWM), Office of Science and Technology and International (OSTI) for their partial funding of this work. My deepest gratitude goes to Martin Piech of United Technologies Research Center; without his expertise, the AFM measurements reported on in this work would never have been completed. I also thank my MS Thesis committee members Rob Bowman, Susan Altman, John Wilson, and Jill Buckley for their guidance and critical review. Last, my ability to complete this work would have been greatly limited without the support of Sandia National Laboratories' Geohydrology Department, particularly Ray Finley, Howard Passell, Susan Altman, and Vince Tidwell.

TABLE OF CONTENTS

LIST OF FIGURES

LIST OF APPENDIX FIGURES

LIST OF TABLES

I. PREFACE

This document is the result of a thesis project completed in partial fulfillment of the requirements for a Master of Science Degree in Hydrology. It includes a manuscript that will be submitted to the Journal of Colloid and Interface Science, as well as supporting appendices.

This work looked at the interaction forces between an environmentally important surface (muscovite mica) and a widely-used model colloid particle (carboxyl-modified polystyrene latex microsphere) using measurements obtained via atomic force microscopy (AFM). The three main objectives of this work were 1) to directly measure the interaction forces between muscovite mica and carboxyl-modified polystyrene latex microspheres, 2) to evaluate the significance of surface charge heterogeneities on the muscovite surface by evaluating AFM measurements taken at several spatial locations, and 3) to evaluate the feasibility of measuring the secondary energy minimum using conventional AFM instrumentation.

This thesis is organized as follows: Section I. Preface describes the objectives of the thesis and its organization. Section II. Manuscript is the draft of a manuscript, entitled "Interaction Forces Measured by Atomic Force Microscopy for Muscovite and Carboxyl-Modified Microspheres as a Function of Ionic Strength", to be submitted to the

Journal of Colloid and Interface Science. Section III. Concluding Remarks presents overall conclusions and recommendations that have resulted from this study. Supporting appendices provide relevant AFM background information (Appendix A: Atomic Force Microscopy Background), additional information on numerical techniques employed as part of the data analysis process (Appendix B: Averaging and Oscillation Removal), results from AFM measurements not included in the manuscript (Appendix C: AFM Measurements Not Reported in the Manuscript), and descriptive information on AFM data (Appendix D: AFM Data). A data CD is included as part of this thesis. Readers unfamiliar with AFM are encouraged to review Appendix A: Atomic Force Microscopy Background before reading the manuscript.

II. MANUSCRIPT

Interaction Forces Measured by Atomic Force Microscopy for Muscovite and Carboxyl-Modified Microspheres as a Function of Ionic Strength

Marissa D. Reno[1,2], Robert S. Bowman[2], and Susan J. Altman[1]

Abstract

This research used atomic force microscopy (AFM) to gain a better understanding of the interactions between muscovite mica and a model colloid used commonly throughout the existing colloid transport literature. The interaction forces between a single crystal muscovite mica disc and a 2.0-μm carboxyl-modified polystyrene latex microsphere attached to a tipless silicon nitride (SiN) cantilever were measured in KCl solutions of varying ionic strength (10, 30, 100, and 300 mM) using AFM. The three main objectives of this work were to 1) directly measure the interaction forces between muscovite mica

[1] Sandia National Laboratories, Geohydrology Department, P.O. Box 5800, Albuquerque, NM 87185-0735

[2] New Mexico Institute of Mining and Technoloy, 801 Leroy Place, Socorro, NM 87801

and carboxyl-modified polystyrene latex microspheres, 2) evaluate the magnitude and significance of surface charge heterogeneities on the muscovite surface by making AFM measurements at several spatial locations, and 3) evaluate the feasibility of measuring the secondary energy minimum using conventional AFM instrumentation. AFM measurements were shown to be qualitatively reproducible only when strict surface preparation techniques were employed and a well-developed experiment protocol was adhered to. For measurements taken at various ionic strengths, repulsive forces were observed to decrease at higher ionic strengths. The tip-sample separation distance at which repulsive forces were first observed increased at lower ionic strengths. Both of these observations are in accord with theoretical predictions of Derjaguin-Landau-Verwey-Overbeek (DLVO) theory. Measurements taken at several spatial locations on the muscovite surface suggested that there is heterogeneity in the muscovite surface properties. This heterogeneity was within the range of forces predicted by DLVO calculations using bounding values of ζ-potential and Hamaker constant. Variability in the tip-sample separation distance at the primary barrier was greater at a lower ionic strength than at a higher ionic strength for both AFM measurements and DLVO predictions. With the instrumentation used in this work, excessive noise and insufficient cantilever sensitivity made measurement of the secondary energy minimum infeasible. The results suggest that AFM is a useful tool for direct measurement of interaction forces and confirmation of theoretical predictions.

Introduction

Subsurface contamination occurs due to natural processes and is exacerbated by anthropogenic sources, including land application of fertilizers and pesticides, accidental chemical spills, general waste disposal practices, and geologic isolation of radioactive waste. Developing sound predictive capabilities and establishing effective methodologies for remediation relies heavily on our ability to understand the physical and chemical mechanisms of contaminant transport in the vadose and saturated zones. Colloids, particles with linear dimensions between 1 and 1000 nm, consisting of natural organic and inorganic materials including viruses, bacteria, humic acids, and mineral fragments, have been identified as a mobile third phase capable of having a significant influence on contaminant transport and mobility in the saturated subsurface (McCarthy and Zachara, 1989). Colloids have thus become integral components of numerous transport studies in both porous and fractured media, gaining much attention because they can move faster than a conservative dissolved species in groundwater, due to charge and size exclusion, and low diffusivity (Bales et al., 1989; Grindrod, 1993; Reimus, 1995; James and Chrysikopoulos, 2003; Sirivithayapakorn and Keller, 2003; Keller et al., 2004). For example, a series of studies have shown that trace metals and radionuclides, which strongly adsorb onto porous media and are generally considered immobile, migrated much further than predicted ignoring the influences of colloids (McKay et al., 1993; Kersting et al., 1999).

Treating colloid transport on the basis of fundamental surface chemical interactions has not been a research area of intense focus. Up until the past few years, most models of

colloid transport have been based on traditional colloid filtration theory (CFT), the original formulation of which came from an attempt to model wastewater filtration processes (Yao et al., 1971). Traditional CFT was developed for saturated, steady-state conditions and utilizes a bulk deposition parameter, the spatially and temporally invariant particle deposition rate coefficient. Several recent studies have suggested that this approach is insufficient. McCarthy and McKay (2004) argued that colloid transport in the vadose zone was a critical area needing investigation. Hahn and O'Melia (2004) made use of the Interaction Force Boundary Layer Model (Speilman and Friedlander, 1974) coupled with Monte Carlo and Brownian Dynamics methods to simulate individual particle trajectories, suggesting that the treatment of colloid transport without consideration of individual particle-surface interactions is insufficient. Several other studies have demonstrated deviations from traditional CFT and suggested that colloid behavior would be more accurately modeled if the mechanisms responsible for the deviations were captured numerically. Colloid deposition in the secondary energy minimum is one of several proposed mechanisms to account for observed deviations from the predictions of traditional colloid filtration and Derjaguin-Landau-Verwey-Overbeek (DLVO) theories (Hahn et al., 2004; Redman et al., 2004; Tufenkji and Elimelech, 2004, 2005; Kuznar and Elimelech, 2007). Deviations have also been shown to arise when steric interactions occur (Tong et al., 2005), when exclusion (Bradford et al., 2003; Tufenkji et al., 2003) or straining (Bradford et al., 2002; Bradford et al., 2003; Tufenkji et al., 2003) mechanisms exist, and for certain experimental transport distances (Bolster et al., 1999). As the body of evidence showing deviations from traditional CFT grows, so

do the number of works proposing mechanisms to explain these deviations. Direct observation of the secondary energy minimum in a model system would be a valuable contribution to understanding colloid attachment and transport phenomena.

Atomic force microscopy (AFM) measurements can facilitate an improved understanding of colloid interactions on a nanometer-scale by employing the colloid probe technique (Ducker et al., 1991). There have already been several applications of this technique in the biological literature (Bowen et al., 1998, 1999; Bowen and Doneva, 2000; Bowen et al., 2002a; Bowen et al., 2002b; Brant and Childress, 2002; Li and Elimelech, 2004; Xu and Logan, 2005; Lee and Elimelech, 2006, 2007) and several applications that suggest usefulness in geologic studies through the use of geologically-relevant probes and substrates (Ducker et al., 1992; Butt et al., 1995; Toikka et al., 1996; Veeramasuneni et al., 1996; Bowen et al., 1999; Lower et al., 2000). To date, little has been done using AFM to investigate the nanoscale interactions between a geologically relevant surface and synthetic latex colloids that are widely used in field and laboratory transport experiments (Harvey et al., 1989; Elimelech and O'Melia, 1990; Toran and Palumbo, 1992; Reimus, 1995). Such direct AFM measurements could facilitate the development of more accurate transport models by providing the parameters (e.g., interaction force as a function of separation distance, derived ζ-potentials) necessary for pore- to nano- scale characterization of colloid-surface interactions.

This work utilized AFM to gain a better understanding of the interactions between muscovite mica, a geologically-relevant mineral surface, and carboxyl-modified polystyrene latex microspheres, which are widely used model colloids. Interaction forces

were measured in potassium chloride (KCl) solutions of varying ionic strength and compared to the predictions of DLVO theory. The objectives of this study were to 1) directly measure the interaction forces between muscovite mica and carboxyl-modified polystyrene latex microspheres, 2) evaluate the magnitude and significance of surface charge heterogeneities on the muscovite surface by making AFM measurements at multiple spatial locations, and 3) evaluate the feasibility of measuring the secondary energy minimum using conventional AFM instrumentation.

Theory

DLVO Predictions

Treating the muscovite-microsphere system as a sphere-plate interaction, the interaction force as a function of the separation distance between the muscovite and the microsphere can be modeled using DLVO theory (Derjaguin and Landau, 1941; Verwey and Overbeek, 1948). For forces acting at a separation distance greater than 0.5 nm, the total interaction energy is the sum of the attractive van der Waals and repulsive electrostatic energies. The attractive van der Waals energy is calculated using the expression proposed by Gregory (1981)

$$W_{vdw} = \left\{-\frac{AR}{6D}\right\}\left[1+\left(\frac{14D}{\lambda}\right)\right]^{-1} \quad (1)$$

where A is the Hamaker constant, R is the sphere radius, D is the distance separating the sphere and the plate, and λ is the characteristic wavelength of the dispersion interaction

and is often taken to be 100 nm (Gregory, 1981). The repulsive electrostatic energy is given by Hogg et al. (1965)

$$W_{EDL} = \pi\varepsilon_0\varepsilon R\left\{2\psi_1\psi_2 \ln\left[\frac{1+\exp(-\kappa D)}{1-\exp(-\kappa D)}\right] + \left(\psi_1^2 + \psi_2^2\right)\ln\left[1-\exp(-2\kappa D)\right]\right\} \qquad (2)$$

where ε_0 is the permittivity of free space (8.854×10^{-12} $C^2J^{-1}m^{-1}$), ε is the dielectric constant of the medium (78.6 for water) (Israelachvili, 1992), ψ_1 and ψ_2 are the surface potentials of the sphere and flat plate, respectively, and κ is the Debye length. The Debye length is calculated as

$$\kappa = \left(\sum_i \rho_{\infty i} e^2 z_i^2 / \varepsilon\varepsilon_0 kT\right)^{1/2} \text{ m}^{-1} \qquad (3)$$

where subscript *i* denotes the ion of interest, ρ_∞ is the number density of ions in the bulk solution, *e* is the elementary charge (1.602×10^{-19} C), and *z* is the valency of ion *i*. Equation (2) only holds exactly for ψ_1 and/or ψ_2 less than 25 mV and for solution conditions such that the double layer thickness is small compared to the particle size. In practice, ζ-potentials are used in the place of surface potentials, due to the fact that surface potentials are not directly measurable. For useful comparison to AFM measurements, the interaction energy is differentiated with respect to separation distance and reported as force in picoNewtons (pN) versus separation distance in nanometers (nm).

A representative example of the forces theoretically predicted by DLVO theory and intuitively comparable to interaction forces measured by AFM is shown in Figure 1.

Repulsive forces are positive, attractive forces are negative, and the total force curve is typified by the existence of a primary force minimum, primary force maximum or barrier, and for certain system chemistry conditions, secondary and tertiary force minima and maxima. Strong repulsion due to steric interactions occurs at a smaller separation distance than the primary minimum; this repulsive portion of the curve is not shown in Figure 1 because applying the scale necessary to view it distorts the labeled features that are of major interest to this work. When the interaction forces resulting from a sphere approaching a plate are observed directly by AFM, only the total force (black line in Figure 1) is captured. Two important differences between the features of a total force curve generated from theoretical DLVO calculations and one measured by AFM are 1) the region of constant compliance and 2) the point of jump-to-contact. The total force curve in Figure 1 suggests that force approaches negative infinity after the primary maximum has been overcome and this is what is labeled as the primary minimum. In reality, and as mentioned previously, an inflection point does in fact exist at a separation distance smaller than that of the primary minimum and strong Born repulsion occurs. This theoretically-predicted repulsion manifests itself in AFM measurements as the region of constant compliance. The region of constant compliance is that portion of an AFM force curve at close separation where a linear relationship exists between force and separation distance and appears as a line with a constant, negative slope. When sufficiently strong attractive forces exist and experimental conditions give rise to a force gradient between the sphere and the plate greater than that of the AFM cantilever spring constant, jump-to-contact occurs. This phenomenon suggests that the interacting surfaces

have overcome the repulsive barrier that separates them. At the jump-to-contact point, AFM output exhibits a sharp discontinuity and shows a significant decrease in force. At lower ionic strengths, a relatively high primary barrier exists and the jump-to-contact force is either relatively weak or does not occur at all, whereas at higher ionic strengths the height of the barrier decreases and the magnitude of the jump-to-contact force increases.

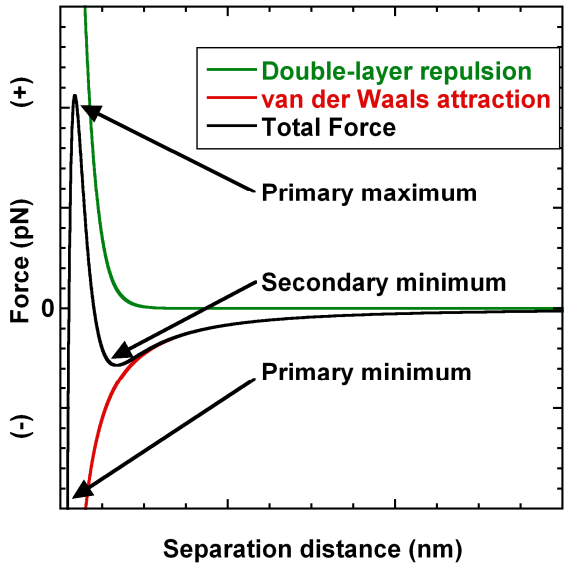

Figure 1: Force versus separation distance for two charged surfaces interacting across an electrolyte solution, after Israelachvili Fig.12.12 (Israelachvili, 1992).

Materials and Methods

Colloid Probes

Surfactant-free fluorescent carboxyl-modified polystyrene latex microspheres with diameters of 2.0 μm (Invitrogen Corporation, product code F8825) were used as model colloids. This particular type of microsphere is widely used in transport studies because it is negatively charged in most natural environments (i.e., dominant –COOH groups deprotonate in solutions with pH greater than 4.5 (Gebhardt and Fuerstenau, 1983)) and it

is readily detectable under a fluorescent microscope. Polystyrene microspheres have been used as tracer particles in aquifer (Harvey et al., 1989) and laboratory column (Toran and Palumbo, 1992) studies, and have also been used to develop and test theoretical numerical formulations of the kinetics of deposition of colloidal particles in porous media (Elimelech and O'Melia, 1990). Carboxyl-modified microspheres are frequently employed in porous media, fracture, and membrane studies (Grolimund et al., 1998; Bradford et al., 2002; Li et al., 2004; Tufenkji and Elimelech, 2005; Kuznar and Elimelech, 2007) and are the primary particle of interest in the theoretical and experimental work of Tufenkji and Elimelech (2004) that elucidates the implications of secondary minimum deposition for colloid transport in porous media.

Colloid probes were prepared by attaching individual microspheres to tipless silicon nitride (SiN) cantilevers with nominal spring constants of 0.32 N/m (Veeco Probes, model number NP-O). Particle mounting, probe calibration, and spring constant determination were performed by Novascan Technologies (Ames, IA). Probes were packed in a dry argon atmosphere and remained in their original container until immediately prior to use. After AFM measurements were complete, the presence of the microsphere was verified by examination under a fluorescent microscope. Figure 2 shows images of a typical colloid probe (a) before and (b) after AFM measurements were conducted. The AFM measurement procedure caused no visible changes in the position of the colloid or the surface of the cantilever.

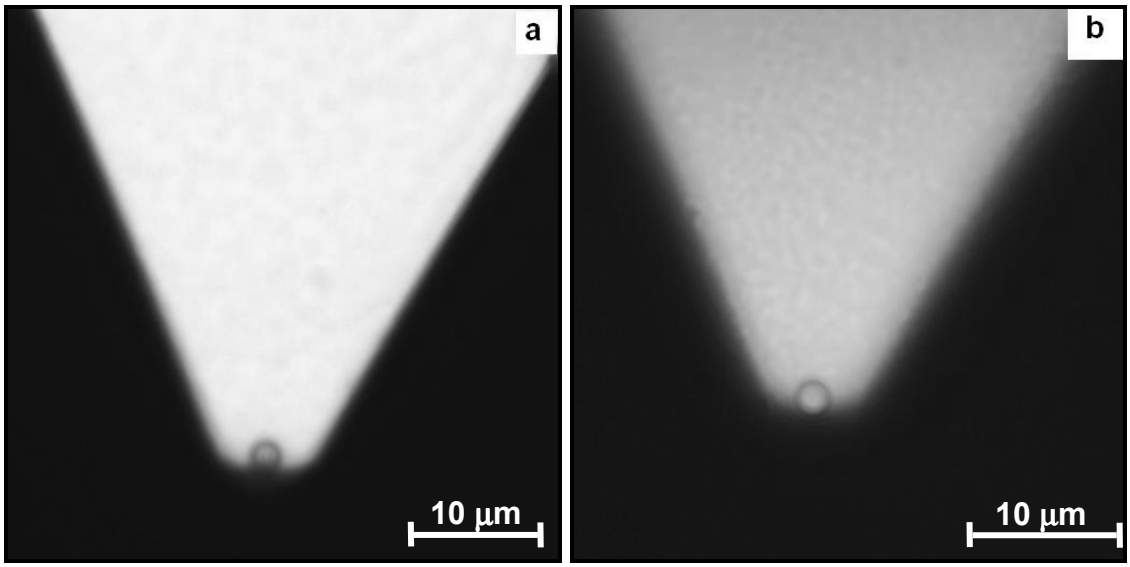

Figure 2: Images of a 2-µm colloid probe before (a) and after (b) AFM measurements were conducted. Figure 2b is darker than 2a because the probe was not completely dry when the image was taken

Mica Surfaces

A grade V-1 single crystal muscovite mica disc of diameter 9.5 mm and thickness 0.15 mm (SPI Supplies, product number 01873-CA) was selected as the substrate for AFM force measurements. Muscovite mica was chosen because it is molecularly smooth, it can be cleaved immediately prior to use thereby minimizing the need for further cleaning, and as a silicate is representative of minerals in natural environments in which colloid transport and interactions are important.

Cleaning Protocol

Every effort was made to minimize contamination of the colloid and muscovite surfaces. General guidelines for preparation of surfaces used in AFM measurements are rare in the literature, likely because the surfaces and systems investigated have been and continue to be diverse such that no one protocol is appropriate for all cases. In a 2001 review of

force microscopy, Senden (2001) called for a comprehensive comparative study of all common cleaning processes; such a study has yet to be completed. Cleaning by UV/ozone exposure (Biggs et al., 2000; Piech and Walz, 2002), rinsing with ethanol (Bowen et al., 1999; Lower et al., 2000; Assemi et al., 2004), and rinsing with deionized or 18 MΩ-cm water (Bowen and Doneva, 2000; Assemi et al., 2004; Lee and Elimelech, 2006) have all been documented, with no justification of the chosen methods. A strict cleaning and preparation protocol was developed for the materials and components specific to the AFM measurement system employed in this work and is reported in detail, as it is anticipated that the information provided will be useful for future studies.

Glass beakers were used as storage containers for clean parts, as reservoirs in which to clean parts, and to transfer 18 MΩ-cm water when preparing electrolyte solutions. Glass bottles with glass stopcocks were used to store prepared electrolyte solutions. All glass materials, with the exception of syringes, were washed in a bath of deionized water and Alconox®, rinsed several times with deionized water until no soap residue remained, and then placed in a 10% HCl bath for at least 180 min. Upon removal from the acid bath, glass parts were rinsed five times with deionized water, followed by copious rinsing with 18 MΩ-cm water, and then placed in a gravity convection oven (Sheldon Manufacturing Inc., Model number 1310) at 105ºF for 24 h. When cool, glass beakers were covered with Parafilm™ and placed upside down in a clean cabinet; glass bottles were capped and placed in the same cabinet. Teflon materials were placed in the same 10% HCl bath for 20 min and rinsed using the same method employed for the glass parts. Teflon materials were dried in the oven at 85ºF. Syringes were cleaned as per the method recommended

by Hamilton Company (Document No. 69051, Rev. F, © Hamilton Company 1/97.). Plungers were removed from the syringe barrel and wiped down with an alcohol wipe, blown dry with filtered dry nitrogen, and then reinserted into syringe barrel. A solution of the Hamilton proprietary Cleaning Concentrate was then pumped through the syringe (3 – 5× volume of syringe), followed by a thorough flushing with 18 MΩ-cm water (10× volume of syringe). The AFM quartz fluid cell and silicone o-ring were cleaned using the method recommended by the manufacturer (2004), which included soaking in warm, soapy water, adding a few drops of liquid dish detergent (Hamilton Cleaning Concentrate used here), gently rubbing with a cotton swab, rinsing copiously with 18 MΩ-cm water, and then blowing dry with filtered dry nitrogen. The fluid cell and o-ring were stored in a clean glass beaker until needed. The colloid probe was cleaned by ethanol rinsing, as described in Atomic Force Microscopy Measurements section. The muscovite substrate, pre-mounted on the AFM sample stage, was cleaved just prior to placing the fluid cell in the AFM head. The system was sealed, as quickly as possible to minimize contamination, by translating the substrate upwards towards fluid cell until in contact with o-ring. This assembled system was then flushed with ethanol, which served as a final cleaning for both the colloid probe and the substrate.

Solution Chemistry

Potassium chloride solutions of ionic strengths 10, 30, 100 and 300 mM were prepared using analytical reagent-grade KCl (Fisher Scientific) and 18 MΩ-cm water. All solutions were adjusted to pH 8 by addition of reagent-grade $KHCO_3$ (Fisher Scientific).

All solutions were prepared in glass containers and stored at room temperature (20 to 21ºC).

Atomic Force Microscopy Measurements

Interaction forces between a 2.0-μm carboxyl-modified microsphere and freshly cleaved single crystal muscovite surface were measured using a NanoScope IIIa MultiMode Atomic Force Microscope (Veeco/Digital Instruments, Santa Barbara, CA). The introduction of and measurement in electrolyte solutions of varying ionic strength was facilitated through the use of a quartz fluid cell and silicone o-ring (Veeco Instruments) with an assembled volume of approximately 1 mL. Teflon inlet and outlet adapters and a Teflon stopcock to prevent backflow of solution were used to facilitate the introduction of solutions. Glass Hamilton Gastight® syringes were used to inject electrolyte solutions.

The experimental protocol for measuring interaction forces involved the following steps: (I) approximately 5 min before initiating the AFM measurement procedure remove single probe from bulk container using tweezers and place in fluid cell; (II) place prepared colloid probe in clean fluid cell; (III) place muscovite disc on AFM sample stage and cleave; (IV) mount the fluid cell in the AFM head, atop the muscovite surface with an o-ring between the two to provide a seal and prevent leakage; (V) bring the muscovite surface and colloid probe into close contact by decreasing the separation distance between the two until the image of the cantilever and the image of the reflection of the cantilever are almost in the same optical plane; (VI) optimize deflection signals; (VII) complete final cleaning step by introducing 3 mL pure ethanol and allowing to remain

stagnant in fluid cell for 1.5 min and then flushing with additional 2 mL; (VIII) flush system with 20 mL of 18 MΩ-cm water; (IX) introduce 10 mL of the 10-mM KCl solution and allow system to equilibrate for 120 min turning laser and microscope light off to minimize heating of system; (X) engage tip and obtain 50 force measurements; (XI) disengage; repeat steps IX through XI for 30-, 100- and 300-mM KCl solutions. The injection volume of 10 mL for all KCl solutions was chosen because it is 10× the volume of the fluid cell-o-ring-muscovite assembly and provided sufficient flushing of the system such that no dilution effects occurred. The equilibration time of 120 min was selected after observing the stability of the system over time. Equilibration times of 30 (Li and Elimelech, 2004), 60 (Lee and Elimelech, 2007), and up to 120 min (Israelachvili and Adams, 1978) have been reported for force measurements in electrolyte solutions.

Three sets of force measurements were obtained on three different days (2 Oct 2006, 4 Oct 2006, and 6 Jan 2007) in order to ensure measurement reproducibility. On any individual day, force measurements were performed at a single location on the muscovite surface with the objective of isolating the effects of varying the ionic strength of the electrolyte solution. For measurements performed on 6 Jan 2007, eight locations were sampled to investigate the significance of surface charge heterogeneities on the muscovite surface. Because measurements taken in the different electrolyte concentrations needed to be at the same location, multiple locations were only sampled at the beginning and end of the series of measurements (i.e., in 10 mM and 300 mM only). The spacing chosen for the surface charge heterogeneity measurements was determined by the expected spacing of discrete mica surface charges from the literature and

instrument constraints. Discrete mica surface charges can range from one charge per 60 nm^2 in a 0.1 mM electrolyte solution to one charge per 0.48 nm^2 in a 100 mM electrolyte solution (Israelachvili and Adams, 1978). For measurements in 10 mM-KCl, four measurements were taken using 120 nm-spacing and an additional four were taken using 60 nm-spacing. For measurements in 300 mM-KCl, one measurement was taken using 4 nm-spacing and seven were taken using 1 nm-spacing.

Results and Discussion

Interaction Forces Predicted by DLVO Calculations

ζ-potentials and Hamaker constants for the muscovite-KCl-carboxyl-modified polystyrene latex microsphere system, hereafter referred to as the muscovite-KCl-microsphere system, were taken from the literature. When only a range was available, maximum and minimum parameter values were used. The ζ-potentials of the microspheres were -60.5, -45.3, -30.1, and -27.9 mV for the 10-, 30-, 100-, and 300-mM KCl solutions, respectively. These values were reported by Tufenkji and Elimelech (2004) in a study that used colloidal particles and electrolyte solutions identical to those utilized in this work. The ζ-potential for the muscovite mica surface was taken to range from -40 to -130 mV based on values reported in the literature (Israelachvili and Adams, 1978; Lyons et al., 1981; Scales et al., 1990) for similar mica surfaces in solutions of like ionic strength and pH. The Hamaker constant for mica-water-polystyrene interactions was taken to range from 1.43 to 1.78×10^{-20} J (Lyklema, 1991).

Solving equations (1) through (3) for the muscovite-KCl-microsphere system gives rise to the curves shown in Figure 3a through Figure 3c. Each plot shows the interaction force in pN versus separation distance in nm.

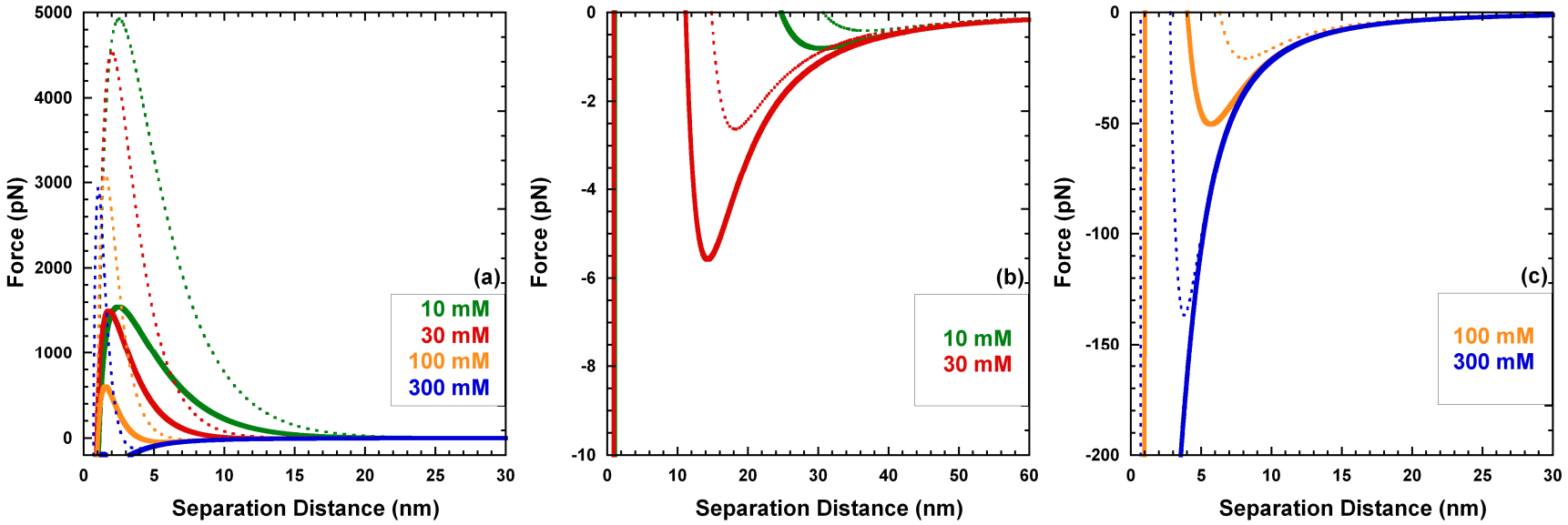

Figure 3: (a) Theoretical force versus separation distance curves for the muscovite-KCl-microsphere system. Two curves are shown at each ionic strength, one dashed line and one solid line of the same color. These are the bounding curves corresponding to ranges of ζ-potential and Hamaker constant taken from the literature. Curves from (a) are shown at a higher resolution for (b) 10 and 30 mM and (c) 100 and 300 mM to emphasize the magnitude and locations of secondary minima.

The interaction force curves in Figure 3a highlight the position and magnitude of the primary force barrier and suggest that the strongest repulsive forces will occur at lower ionic strengths, decreasing at higher ionic strengths. In fact, the lower bounding case for interactions at 300 mM predicts completely attractive forces (Figure 3c). If direct AFM measurements are in agreement with these theoretical predictions, an increase in the magnitude of the jump-to-contact force should be observed at higher ionic strengths. Furthermore, the separation distance at which repulsive forces are first felt should increase at lower ionic strengths, in accord with the expansion of the electrostatic double layers.

Secondary minima are highlighted in Figure 3b and Figure 3c. The depth of the secondary minimum is greater at higher ionic strengths and might not exist at 300 mM, depending on the ζ-potential and Hamaker constant values assumed in the calculations, as seen by the lower bounding case in Figure 3c. The separation distance at which the secondary minimum occurs is predicted to decrease at higher ionic strengths.

The theoretical occurrence of the primary barrier and secondary minimum does not ensure that they will be detected by AFM. The sensitivity of the instrument and/or measurement technique must be considered. Forces as small as 10^{-6} pN have been proposed to be measurable by AFM based on the force needed to move a cantilever beam with an ultrasmall mass attached (Binnig et al., 1986). However, in practice, forces on the order of 2 pN are the smallest reported (Piech and Walz, 2002). This sensitivity required that extensive measures be taken to minimize environmental noise and that highly specialized cantilevers with minimal spring constants, only available for use with

particles approximately 10-μm and greater in diameter, be utilized. Based on previous works that did not go to extensive measures to maximize sensitivity, it is expected that forces of magnitude greater than 40 to 70 pN should be readily measurable by AFM (Butt, 1991; Biggs et al., 2000). Theoretical calculations (Figure 3a through Figure 3c) suggest that all primary force barriers, ranging from 600 to 5000 pN, should be measurable. The secondary minimum will however only be detectable for certain ionic strength conditions. For interactions in 300-mM KCl, the predicted secondary minimum is expected to be detectable at approximately 120 pN for the upper bounding case; otherwise there is no secondary minimum. For interactions in 100-mM KCl, detection is more likely if forces fall along the lower predicted bound (50 pN) than the upper predicted bound (20 pN). For interactions in 30- and 10-mM KCl, detection of secondary minima is unlikely since all are predicted to be very close to the minimum threshold obtainable after significant sensitivity-maximizing efforts, as reported by Piech and Walz (2002).

Atomic Force Microscopy Data Analysis

Raw AFM data, deflection voltage versus sample displacement, were converted to force versus tip-sample separation distance using the method described by Ducker et al. (1992). This method requires that the tip-sample separation distance corresponding to zero separation distance and force corresponding to zero force be determined and specified by the data analyst. Zero separation is determined by first calculating the tip-sample separation distance over the entire profile, which requires summing sample-displacement due to the movement of the AFM scanner and tip-displacement resulting from the

deflection of the cantilever, and then taking the average of this distance over the region of constant compliance. The force at which zero force occurs is given by the average deflection signal when the interacting surfaces are far apart. Additional steps were necessary to convert the data presented in this work from deflection voltage versus sample displacement to force versus tip-sample separation distance.

Each set of force measurements for any given KCl solution had 50 associated raw AFM data files, which provided deflection in volts (V) versus sample displacement in nanometers (nm). Each of the 50 deflection versus sample displacement curves was aligned in the x- and y-directions and averaged. The average deflection versus sample displacement curve was then corrected to eliminate oscillations present due to optical interference.

Optical interference has been noted by other researchers (Piech and Walz, 2002; Li and Elimelech, 2004) and arises because of the path difference between the part of the incident laser beam reflected off of the cantilever and the part reflected off of the sample surface. When the two beams recombine in the photodiode detector, an interference pattern forms that is superimposed on top of the measured deflection signal. The resulting oscillations in the baseline of the deflection versus sample displacement plot can be removed by fitting a wave function of the form

$$a + \left[b \times \exp\left(-x/f\right) \times \sin\left(2\pi x/c + d\right)\right] + ex \tag{4}$$

where a is the amplitude offset, b is the amplitude, x is the sample displacement, f is a decay constant, c is ½ the period, d is the phase shift, and e is the slope of a line

representative of the linear trend in the data. This function was chosen because it includes a sine term to account for the interferometer waveform (Born and Wolf, 1999) and a linear offset term to account for drift. Figure 4 shows an example of (a) an uncorrected average deflection signal and (b) the signal after corrected for optical interference.

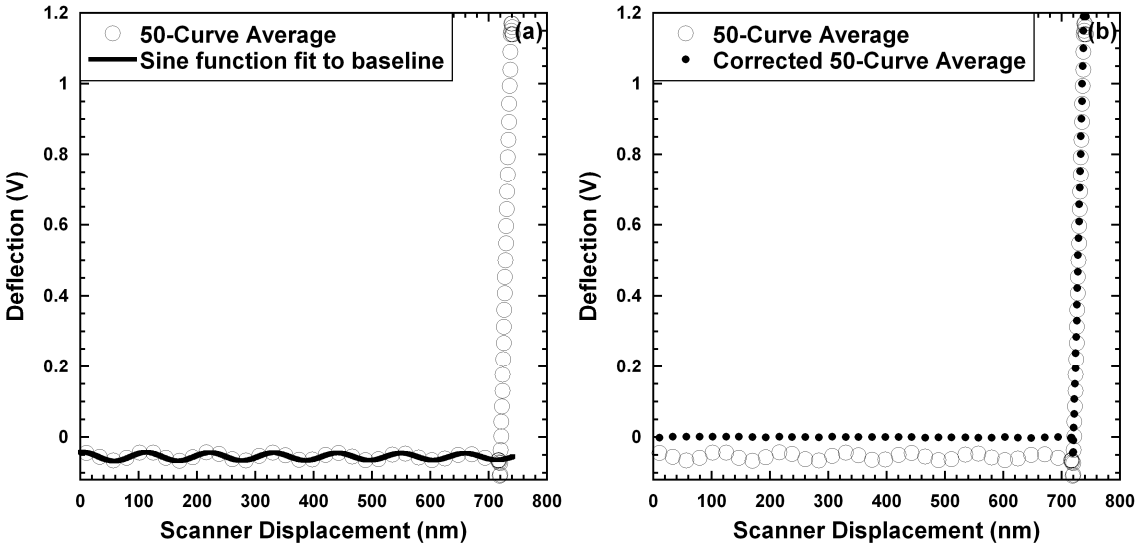

Figure 4: Example deflection vs. sample displacement plots showing (a) raw data with the fitted sine function of (4) and (b) data before and after oscillation removal (data from 4 Oct 2006, 100-mM KCl).

When the amplitude of the oscillation was greater than 10% of the depth of the jump-to-contact portion of the individual deflection versus sample displacement curve, it was necessary to correct for the oscillations before averaging the curves; failure to do so gave rise to an underestimation of interaction forces. For the 22 sets of force measurements collected in this work, only one set (data collected in 100 mM KCl on 4 Oct 2006) exhibited oscillation amplitude greater than 10% of the jump-to-contact depth. For this set of 50 curves, oscillations were subtracted for each curve individually, and then the oscillation-free curves aligned and averaged. All other data sets were

analyzed by averaging raw curves first, subtracting oscillations from the average, and calculating force versus tip-sample separation distance. For a full discussion of the most appropriate averaging technique for a given curve see Reno (2007). After the oscillation-free average had been calculated, force versus tip-sample separation distance curves were generated.

Interaction Forces From AFM Measurements

Direct AFM observations for the muscovite-KCl-microsphere system are shown in Figure 5 and Figure 6. Secondary minima were not observed in any of the measurements. For AFM measurements made in 10-mM KCl, repulsive forces were sufficiently strong such that no jump-to-contact was observed. For measurements made in 30-, 100-, and 300-mM KCl, the primary maxima were overcome and jump-to-contact occurred.

Figure 5 gives results from force measurements obtained on 2 Oct 2006 (a), 4 Oct 2006 (b), and 6 Jan 2007 (c). For the muscovite-KCl-microsphere system and experimental protocol detailed in this work, AFM measurements were qualitatively reproducible between the different times of measurements. The strongest repulsive forces occurred in the 10-mM KCl solution, with repulsion decreasing and forces becoming strongly attractive as ionic strength of the KCl solution increased to 300 mM. This pattern was seen on each of the three measurement days; however, the magnitude of the jump-to-contact forces corresponding to each ionic strength varied. Variations were generally less than 100 pN and likely attributable to minor changes in the system from day to day (e.g., new muscovite surfaces and colloid probes). These variations captured spatial variability in addition to probe-substrate variability.

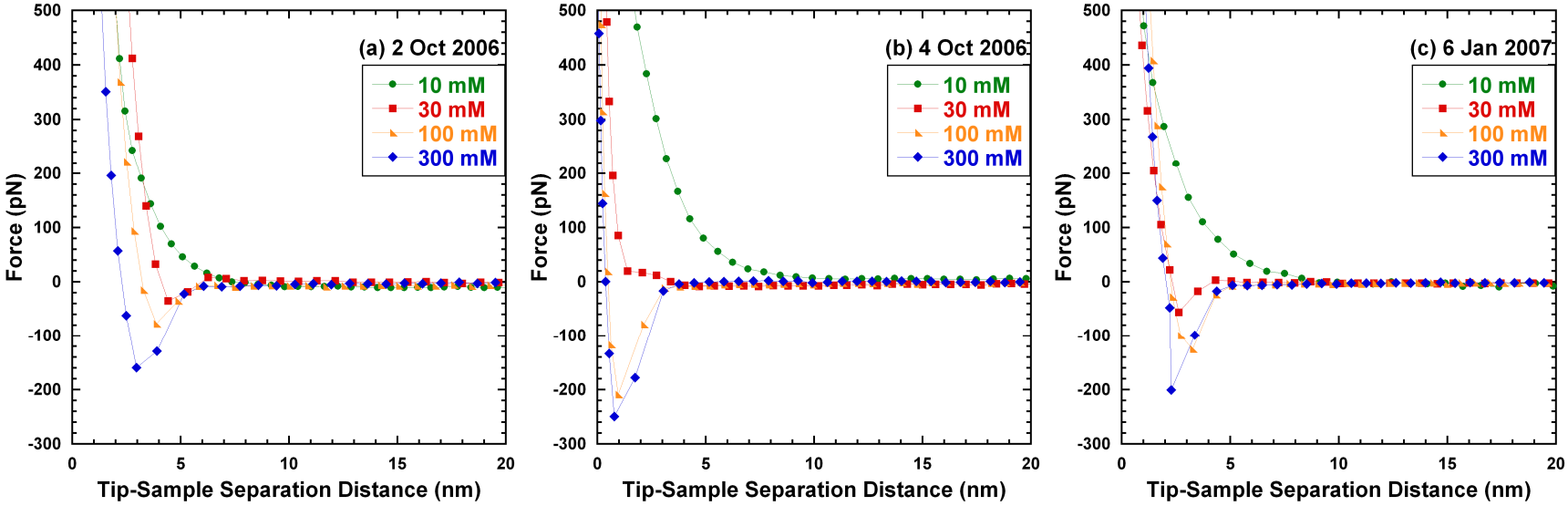

Figure 5: AFM measurements for the muscovite-KCl-microsphere system. Identical measurements were performed on three different days. (a) 2 Oct 2006. (b) 4 Oct 2006. (c) 6 Jan 2007. A new muscovite surface and colloid probe were used on each day. Each curve is the corrected average of 50 individual force measurements.

The tip-sample separation distance at which contact occurs in Figure 5a through 5c not only appears to occur at a distance as large as 4 nm for interactions in 30-mM KCl on 2 Oct 2006, but also to vary from day to day for interactions in like ionic strength solutions. It is important to note that tip-sample separation distance is not absolute. Instead, it is a measure relative to zero separation (i.e., the distance of zero separation is subtracted from all measured tip-sample separation distances). Recall that zero separation is the average of the tip-sample separation distance over the region of constant compliance. For compressible surfaces, true physical contact occurs before constant compliance occurs, resulting in a zero separation distance value smaller than the true value. It is therefore not surprising that Figure 5 shows contact occurring at tip-sample separation distances greater than zero. The apparent day to day variation in the distances is also reasonable if the relationship between applied load, deformation of one or both of the surfaces, and constant compliance is considered, where inconsistent force applied at contact will result in an inconsistent definition for the region of constant compliance (Ralston et al., 2005). For the measurements being compared in Figure 5a through 5c, maintaining a constant applied load was not possible due to slight variations in the system from day to day influencing the deflection setpoint. Given the imprecise nature of defining zero separation, it is reasonable that the tip-sample separation distance at contact was not only greater than zero, but varied from day to day for interactions in like ionic strength solutions.

Results shown in Figure 5 also demonstrate qualitative agreement with theoretical DLVO predictions. Repulsive forces are strongest at lower ionic strengths, decreasing at higher

ionic strengths. Note the increase in the magnitude of the jump-to-contact force as ionic strength increases. The separation distance at which the repulsive force is felt also shows qualitative agreement with theoretical predictions, increasing at lower ionic strengths. This pattern is particularly apparent for the 2 Oct 2006 data.

Figure 6 shows results from measurements taken at eight spatial locations on a single muscovite surface on 6 Jan 2007 in an effort to evaluate the significance of surface charge heterogeneities. Theoretical calculations (Figure 3a) suggest that variations in the height of the primary maximum, or depth of the jump-to-contact point as it is observed with AFM, and the separation distance at which the primary force barrier is first felt should be larger at lower ionic strengths.

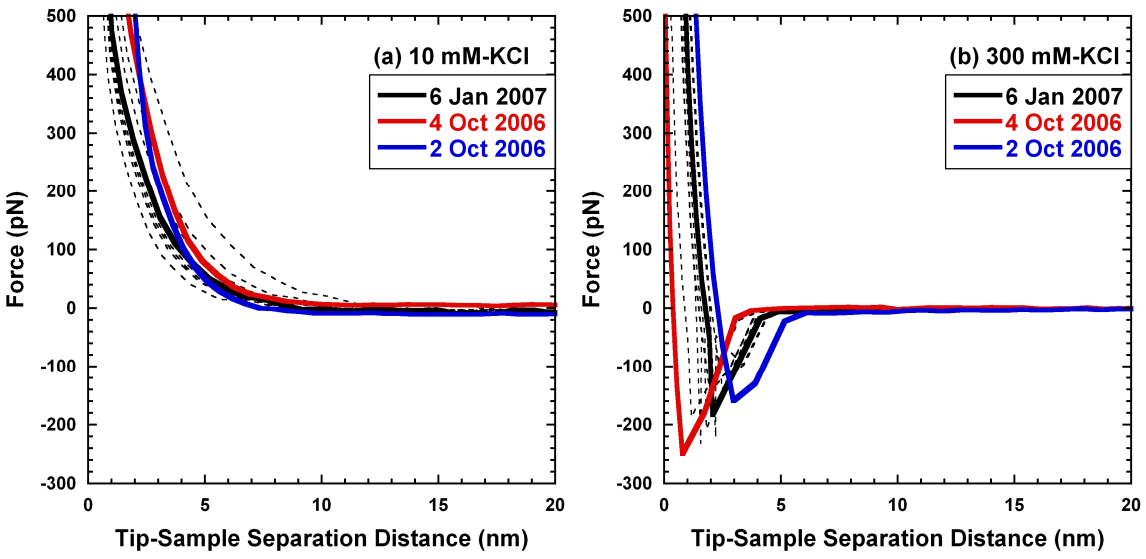

Figure 6: Spatial heterogeneity of AFM measurements for the muscovite-KCl-microsphere system. (a) 10-mM KCl. (b) 300-mM KCl. Thick solid lines are same data as shown in Figure 5 for the three measurement days. Thin dashed lines are from data collected on 6 Jan 2007 at different locations on a single muscovite surface. Each curve is the corrected average of 50 individual force measurements.

The forces shown in Figure 6 agree with predictions, as evident by measurements made at 10-mM KCl showing greater variations in the separation distance where the force of

the primary barrier was first felt than the same variations at 300 mM. It is also interesting to note that for 300-mM KCl, measured spatial variation is encompassed by measured probe-substrate variation, while this is not the case for 10-mM KCl. The various spacing intervals employed had no systematic impact on measured forces. Table 1 summarizes the range of theoretically-predicted primary maxima forces and directly observed jump-to-contact forces. Recall that the DLVO calculations provide the height of the primary force barrier, whereas AFM measurements made in this work only provide the depth of the jump-to-contact point. Therefore, to compare the two sets of force values, a relationship between the height of the primary force barrier and the depth of the jump-to-contact point must be conjectured. The higher the force barrier, the greater the repulsive force and the smaller the force will be at jump-to-contact. For measured interaction forces in 10-mM KCl, the height of the force barrier is taken to be infinite, as measurements indicate a purely repulsive interaction. For theoretically predicted forces in 300-mM KCl, the lower bounding case suggests purely attractive forces, hence there is no primary barrier. The forces shown in Table 1 reinforce the point that a higher theoretical primary barrier indicates stronger physical repulsion, and therefore a lower jump-to-contact force measured with AFM. Absolute quantitative agreement is not expected, as the force of the primary barrier and the force of jump-to-contact point are not one and the same; however, also evident is the lack of relative quantitative agreement between AFM measurements and theoretical predictions. Theoretical forces exhibit a force gradient at least one order of magnitude greater than the same gradient for forces measured by AFM. This comparison suggests that neither a direct nor indirect

quantitative relationship can be established between theoretically predicted forces and the forces measured by AFM in this work.

KCl (mM)	Measured Jump-to-Contact Forces (pN)		Theoretically Predicted Primary Maxima Forces (pN)	
	Min	Max	Min	Max
10	∞	∞	1546	4900
30	35	56	1499	4500
100	77	160	603	3100
300	160	250	0	2900

Table 1: Summary of measured jump-to-contact forces and theoretically predicted primary maxima forces for the muscovite-KCl-microsphere system.

AFM Measurement Sensitivity

Force measurements for the muscovite-KCl-microsphere system employed in this work were subject to two major and readily identifiable factors that constrained the achievable sensitivity: noise in the baseline data from oscillations introduced by optical interference and the sensitivity of the chosen cantilever.

Oscillation amplitude ranged from 2 to 6 pN for the data collected in this study. This suggests that when oscillations were removed (see Figure 4), a force ranging from 2 to 6 pN was subtracted from every single force value. This oscillation amplitude range applied to different sets of measurements; for any one set of measurements, the amplitude was constant. Recalling that the DLVO theory predicts secondary minima less than 6 pN for interactions in 30- and 10-mM KCl (see Figure 3b), it is reasonable that no secondary minima were observed for the muscovite-KCl-system at these two ionic strengths. This conjecture assumes that the jump-to-contact point occurred at the peak of an optical oscillation, meaning that the physical force from the muscovite-microsphere interaction

would equal a maximum of -6 pN and optical interference could give rise to an equal and opposite signal of 6 pN. When this oscillation with a 6-pN amplitude was subtracted from the entire force curve, it would negate the -6-pN force of the secondary minimum. For interactions in 100- and 300-mM KCl, the range of forces for the predicted secondary minima (see Figure 3c) shows significantly larger values than the force of the oscillations; it is therefore likely that the absence of secondary minima in the AFM force measurements is not due to these forces being overwhelmed by optical interference, but instead is attributable to the use of a cantilever of insufficient responsiveness.

At the time that these measurements were performed, the SiN cantilevers, to which the carboxyl-modified microspheres were attached, were available with cantilever spring constants of 0.06 N/m or 0.32 N/m. The stiffer cantilever was chosen to reduce the impact of baseline noise (e.g., thermal, mechanical, and acoustical vibrations) and maximize the likelihood of obtaining measurements that demonstrated reproducibility. This objective was achieved (see Figure 5). With a cantilever of this spring constant, the minimum measured force, considering all measurements made for this study, was 43 pN (0.023 N/m), achieved in 30-mM KCl on 2 Oct 2006. Theoretical DLVO predictions for interactions in 100-mM and 300-mM KCl suggest that sensitivities of 0.002 and 0.0008 N/m are needed to detect secondary forces at these two ionic strengths. In other words, sensitivity must be improved by at least one order of magnitude relative to the sensitivity achieved with the instrumentation used in this study. Keep in mind that sensitivity is not equivalent to the cantilever spring constant; it is a combination of the cantilever spring constant, instrument settings, and environmental factors. Therefore, in

order to achieve the necessary sensitivity, not only does a cantilever of lower spring constant need to be employed, but further steps need to be taken to optimize instrument settings, minimize environmental noise, and physically eliminate optical interference. Optimization of instrument settings would require steps beyond those traditionally employed to obtain a force curve that looks reasonable as viewed using the Nanoscope software. Additional steps would include a systematic evaluation of the impact of scan rate, ramp size, and Z-limit on measured forces and optimization of these parameters. Elimination of optical interference would likely require the employment of an incoherent light source.

Conclusions

Atomic force microscopy (AFM) and the colloid probe technique were used to investigate the interaction between freshly cleaved muscovite mica and carboxyl-modified polystyrene latex microspheres in KCl solutions of varying ionic strength. Measurements taken on three different days and employing the identical experiment protocol yielded results that were qualitatively reproducible, lending confidence to the experimental technique and observed force interactions. Repulsive forces diminished at higher ionic strengths and the separation distance at which repulsive forces were first encountered occurred at a larger separation for lower ionic strengths. These results are in agreement with the predictions of DLVO theory. AFM measurements taken at multiple spatial locations on the muscovite surface reflected the heterogeneity inherent in the mineral surface. At low ionic strength, the spatial heterogeneity observed for a single muscovite surface was greater than the combined

probe-substrate and spatial variability. At high ionic strength, combined probe-substrate and spatial variability was greater than the spatial heterogeneity observed for a single muscovite surface. Observed variability was greater than the minimum measured force of 43 pN achieved in this study, lending confidence that the variability was due to physical characteristics of the muscovite surface, not noise inherent in the AFM system. All measured spatial variability was at least an order of magnitude lower than that predicted by theoretical calculations; however, qualitative relationships do hold, with variation in the separation distance at which the force of the primary barrier is first felt being greater at 10-mM KCl than at 300-mM KCl. Though theoretically measurable for some of the solution conditions tested here, the secondary energy minimum was not observed, likely due to excessive environmental noise and a cantilever of insufficient sensitivity. The success of previous researchers in employing relatively simple measurement techniques and consistently measuring forces ranging from 40 to 70 pN (Butt, 1991; Biggs et al., 2000) lends confidence that the primary and secondary force maxima and minima for muscovite and carboxyl-modified polystyrene latex microspheres in 100- and 300-mM KCl, can be readily measured by AFM. Furthermore, with extremely careful efforts to maximize sensitivity, it should be feasible to measure these same interaction forces in 30-mM KCl based on the sensitivity of 2 pN reported by Piech and Walz (2002). It is unlikely that forces in 10-mM KCl can be measured using existing AFM instrumentation. Because colloid interactions in environmental waters of high ionic strength pose and interesting problem and have yet to be fully understood, it is concluded that refinement of the techniques presented here (i.e., minimization of noise

and maximization of sensitivity by utilizing a more responsive cantilever) would be a worthwhile effort and could yield very accurate information on the interaction forces between muscovite mica and carboxyl-modified polystyrene latex microspheres in high ionic strength environments, providing insight for and input to numerical models seeking to represent colloidal interactions with geologic media at the nanoscale. It is important to note however that numerical representations requiring absolute separation distances will not be able to utilize the force-distance data provided by AFM.

Acknowledgements

This work was funded in part by Sandia National Laboratories' Laboratory Directed Research and Development (LDRD) program. This work was also partially supported by the Department of Energy, Office of Civilian Radioactive Waste Management (OCRWM), Office of Science and Technology and International (OSTI). Sandia is a multiprogram laboratory operated by Sandia Corporation, a Lockheed Martin Company for the United States Department of Energy's National Nuclear Security Administration under contract DE-AC04-94AL85000.

References

Veeco Instruments Inc., *MultiMode SPM Instruction Manual*, 2004.

Assemi, S., P. G. Hartley, P. J. Scales, and R. Beckett, 2004. Investigation of adsorbed humic substances using atomic force microscopy, *Colloid Surface A*, **248**, 17-23.

Bales, R. C., C. P. Gerba, G. H. Grondin, and S. L. Jensen, 1989. Bacteriophage transport in sandy soil and fractured tuff, *Appl. Environ. Microb.*, **55(8)**, 2061-2067.

Biggs, S., J. L. Burns, Y. Yao-de, G. J. Jameson, and P. Jenkins, 2000. Molecular Weight Dependence of the Depletion Interaction between Silica Surfaces in Solutions of Sodium Poly(styrene sulfonate), *Langmuir*, **16**, 9242-9248.

Binnig, G., C. F. Quate, and C. Gerber, 1986. Atomic Force MIcroscope, *Phys. Rev. Lett.*, **56**(9),

Bolster, C. H., A. L. Mills, G. M. Hornberger, and J. S. Herman, 1999. Spatial distribution of deposited bacteria following miscible displacement experiments in intact cores, *Water Resour. Res.*, **35**(6), 1797-1807.

Born, M., and E. Wolf, 1999, *Principles of optics*, Cambridge University Press, Cambridge, UK.

Bowen, W. R., and T. Doneva, 2000. Atomic Force Microscopy Studies of Membranes: Effect of Surface Roughness on Double-Layer Interactions and Particle Adhesion, *J. Colloid Interface Sci.*, **229**, 544-549.

Bowen, W. R., T. Doneva, and A. G. Stoton, 2002a. The use of atomic force microscopy to quantify membrane surface electrical properties, *Colloid Surface A*, **201**, 73-83.

Bowen, W. R., A. S. Fenton, R. W. Lovitt, and C. J. Wright, 2002b. The Measurement of *Bacillus mycoides* Spore Adhesion Using Atomic Force Microscopy, Simple Counting Methods, and a Spinning Disk Technique, *Biotechnol Bioeng*, **79**(2),

Bowen, W. R., N. Hilal, R. W. Lovitt, and C. J. Wright, 1998. A new technique for membrane characterisation: direct measurement of the force of adhesion of a single particle using an atomic force microscope, *J. Membrane Sci*, **139**, 269-274.

Bowen, W. R., N. Hilal, R. W. Lovitt, and C. J. Wright, 1999. An atomic force microscopy study of the adhesion of a silica sphere to a silica surface--effects of surface cleaning, *Colloid Surface A*, **157**, 117-125.

Bradford, S. A., J. Simunek, M. Bettahar, M. T. Van Genuchten, and S. R. Yates, 2003. Modeling Colloid Attachment, Straining, and Exclusion in Saturated Porous Media, *Environ. Sci. Technol.*, **37**, 2242-2250.

Bradford, S. A., S. R. Yates, M. Bettahar, and J. Simunek, 2002. Physical factors affecting the transport and fate of colloids in saturated porous media, *Water Resour. Res.*, **38**(12), **63**-**6**1-**63**-12.

Brant, J. A., and A. E. Childress, 2002. Membrane-Colloid Interactoins: Comparison of Extended DVLO Predictions with AFM Force Measurments, *Environ. Eng. Sci.*, **19**(6), 413-427.

Butt, H.-J., 1991. Measuring electrostatic, van der Waals, and hydration forces in electrolyte solutions with an atomic force microscope, *Biophys. J.*, **60**, 1438-1444.

Butt, H.-J., J. Manfred, and W. A. Ducker, 1995. Measuring surface forces in aqueous electrolyte solution with the atomic force microscope, *Bioelectroch. Bioener* . **38**, 191-201.

Derjaguin, B. V., and L. Landau, 1941. *Acta Phys. Chim*, **14**(633-662),

Ducker, W. A., T. J. Senden, and R. M. Pashley, 1991. Direct measurement of colloidal forces using an atomic force microscope, *Nature*, **353**, 239-241.

Ducker, W. A., T. J. Senden, and R. M. Pashley, 1992. Measurment of Fores in Liquids Using a Force Microscope, *Langmuir*, **8**, 1831-1836.

Elimelech, M., and C. R. O'Melia, 1990. Kinetics of Deposition of Colloidal Particles in Porous Media, *Environ. Sci. Technol.*, **24**, 1528-1536.

Gebhardt, J. E., and D. W. Fuerstenau, 1983. Adsorption of polyacrylic acid at oxide/water interfaces, *Colloid Surface*, **7**(3), 221-231.

Gregory, J., 1981. Approximate Expressions for Retarded van der Waals Interaction, *J. Colloid Interface Sci.*, **83**(1), 138-145.

Grindrod, P., 1993. The impact of colloids on the migration and dispersal of radionuclides within fractured rock, *J. Contam. Hydrol.*, **13**, 167-191.
Grolimund, D., M. Elimelech, M. Borkovec, K. Barmettler, R. Kretzschmar, and H. Sticher, 1998. Transport of in Situ Mobilized Colloidal Particles in Packed Soil Columns, *Environ. Sci. Technol.*, **32**, 3562-3569.
Hahn, M. W., D. Abadzic, and C. R. O'Melia, 2004. Aquasols: On the Role of Secondary Minima, *Environ. Sci. Technol.*, **38**, 5915-5924.
Hahn, M. W., and C. R. O'Melia, 2004. Deposition and Reentrainment of Brownian Particles in Porous Media under Unfavorable Chemical Conditions: Some Concepts and Applications, *Environ. Sci. Technol.*, **38**, 210-220.
Harvey, R. W., L. H. George, R. L. Smith, and D. R. LeBlanc, 1989. Transport of Microspheres and Indigenous Bacteria through a Sandy Aquifer: Results of Natural- and Forced-Gradient Tracer Experiments, *Environ. Sci. Technol.*, **23**, 51-56.
Hogg, R., T. W. Healy, and D. W. Fuerstenau, 1965. Mutual Coagulation of Colloidal Dispersions, *T Faraday Soc.*, **66**, 1638-1651.
Israelachvili, J., 1992, *Intermolecular and Surface Forces*, Elsevier, London.
Israelachvili, J. N., and G. E. Adams, 1978. Measurement of forces between two mica surfaces in aqueous electrolyte solutions in the range 0–100 nm, *J. Chem. Soc., Faraday Trans. 1*, **74**, 975-1001.
James, S. C., and C. V. Chrysikopoulos, 2003. Effective velocity and effective dispersion coefficient for finite-sized particles flowing in a uniform fracture, *J. Colloid Interface Sci.*, **263**, 288-295.
Keller, A. A., S. Sirivithayapakorn, and C. V. Chrysikopoulos, 2004. Early breakthrough of colloids and bacteriophage MS2 in a water-saturated sand column, *Water Resour. Res.*, **40**,
Kersting, A. B., D. W. Efurd, D. L. Finnegan, D. J. Rokop, D. K. Smith, and J. L. Thompson, 1999. Migration of plutonium in ground water at the Nevada Test Site, *Nature*, **397**, 56-59.
Kuznar, Z., and M. Elimelech, 2007. Direct Microscopic Observation of Particle Deposition in Porous Media: Role of the Secondary Energy Minimum, *Colloid Surface A*, **294**, 156-162.
Lee, S., and M. Elimelech, 2006. Relating Organic Fouling of Reverse Osmosis Membranes to Intermolecular Adhesion Forces, *Environ. Sci. Technol.*, **40**, 980-987.
Lee, S., and M. Elimelech, 2007. Salt cleaning of Organic-Fouled Reverse Osmosis Membranes, *Water Res.*, **41**, 1134-1142.
Li, Q., and M. Elimelech, 2004. Organic Fouling and Chemical Cleaning of Nanofiltration Membranes: Measurements and Mechanisms, *Environ. Sci. Technol.*, **38**, 4683-4693.
Li, X., T. D. Scheibe, and W. P. Johnson, 2004. Apparent Decreases in Colloid Deposition Rate Coefficients with Distance of Transport under Unfavorable Deposition Conditions: A General Phenomenon, *Environ. Sci. Technol.*, **38**, 5616-5625.

Lower, S. K., C. J. Tadanier, and M. F. Hochellla, 2000. Measuring interfacial and adhesion forces between bacteria and mineral surfaces with bilogical force microscopy, *Geochimica et Cosmochimica Acta*, **64**(18), 3133-3139.

Lyklema, J., 1991, *Fundamentals of Interface and Colloid Science*, Academic Press, London.

Lyons, J. S., D. N. Furlong, and T. W. Healy, 1981. The Electrical Double-Layer Properties of the Mica (Muscovite)-Aqueous Electrolyte Interface, *Aust J. Chem*, **34**, 1177-1187.

McCarthy, J. F., and L. D. McKay, 2004. Colloid Transport in the Subsurface: Past, Present, and Future Challenges, *Vadose Zone J.*, **3**, 326-337.

McCarthy, J. F., and J. M. Zachara, 1989. Subsurface transport of contaminants, *Environ. Sci. Technol.*, **23**(5), 495-502.

McKay, L. D., R. W. Gillham, and J. A. Cherry, 1993. Field experiments in fractured clay till: 2. Solute and colloid transport, *Water Resour. Res.*, **20**, 1149-1162.

Piech, M., and J. Y. Walz, 2002. Direct measurement of depletion and structural forces in polydisperse, charged systems, *J. Colloid Interface Sci.*, **253**(1), 117-129.

Ralston, J., I. Larson, M. W. Rutland, A. A. Feiler, and M. Klein, 2005. Atomic Force Microscopy and Direct Surface Force Measurements, *Pure Appl. Chem.*, **77**(12), 2149-2170.

Redman, J. A., S. A. Walker, and M. Elimelech, 2004. Bacterial Adhesion and Transport in Porous Media: Role of the Secondary Energy Minimum, *Environ. Sci. Technol.*, **38**, 1777-1785.

Reimus, P. W., Transport of Synthetic Colloids through Single Saturated Fractures: A Literature Review, LA-12707-MS, Los Alamos National Laboratory, 1995.

Reno, M. D., Interaction Forces Measured by Atomic Force Microscopy for Muscovite and Carboxyl-Modified Microspheres as a Function of Ionic Strength, M.S. Thesis, New Mexico Institute of Mining and Technology, 2007.

Scales, P. J., F. Grieser, and T. W. Healy, 1990. Electrokinetics of the Muscovite Mica-Aqueous Solution Interface, *Langmuir*, **6**(3), 582-589.

Senden, T. J., 2001. Force microscopy and surface interactions, *Curr. Opin. Colloid In.*, **6**, 95-101.

Sirivithayapakorn, S., and A. Keller, 2003. Transport of colloids in saturated porous media: A pore scale observation of the size exclusion effect and colloidal acceleration, *Water Resour. Res.*, **39**(4),

Speilman, L. A., and S. K. Friedlander, 1974. Role of Electrical Double Layer in Particle Deposition by Convective Diffusion, *J. Colloid Interface Sci.*, **46**(1), 22-31.

Toikka, G., R. A. Hayes, and J. Ralston, 1996. Adhesion of Iron Oxide to Silica Studied by Atomic Force Microscopy, *J. Colloid Interface Sci.*, **180**, 329-338.

Tong, M., T. A. Camesano, and W. P. Johnson, 2005. Spatial Variation in Deposition Rate Coefficients of an Adhesion-Deficient Bacterial Strain in Quartz Sand, *Environ. Sci. Technol.*, **39**, 3679-3687.

Toran, L., and A. V. Palumbo, 1992. Colloid transport through fractured and unfractured laboratory sand columns, *J. Contam. Hydrol.*, **9**, 289-303.

Tufenkji, N., and M. Elimelech, 2004. Deviation from the Classical Colloid Filtration Theory in the Presence of Repulsive DLVO Interactions, *Langmuir*, **20**(25), 10818-10828.

Tufenkji, N., and M. Elimelech, 2005. Breakdown of Colloid Filtration Theory: Role of the Secondary Energy Minimum and Surface Charge Heterogeneities, *Langmuir*, **21**, 841-852.

Tufenkji, N., J. A. Redman, and M. Elimelech, 2003. Interpreting Deposition Patterns of Microbial Particles in Laboratory-Scale Column Experiments, *Environ. Sci. Technol.*, **37**, 616-623.

Veeramasuneni, S., M. R. Yalamanchili, and J. D. Miller, 1996. Measurement of Interaction Forces between Silica and α-Alumina by Atomic Force Microscopy, *J. Colloid Interface Sci.*, **184**, 594-600.

Verwey, E. K. W., and J. T. G. Overbeek, 1948, *Theory of Stability of Lyophobic Colloids*, Elsevier, Amsterdam.

Xu, L.-C., and B. E. Logan, 2005. Interaction Forces between Colloids and Protein-Coated Surfaces Measured Using an Atomic Force Microscope, *Environ. Sci. Technol.*, **39**, 3592-3600.

Yao, K.-M., M. T. Habibian, and C. R. O'Melia, 1971. Water and Waste Water Filtration: Concepts and Applications, *Environ. Sci. Technol.*, **5**(11), 1105-1112.

III. CONCLUDING REMARKS

Beyond the conclusions presented in the manuscript, several other important points deserve to be highlighted: 1) surface preparation techniques, 2) instrument setting optimization, and 3) data analysis technique.

In many AFM studies, discussion of surface preparation is given cursory treatment or is neglected all together. This is not to say that researchers are neglecting careful surface preparation procedures, simply that they are neglecting to report their methods. In a review of force microscopy, Senden (2001) called for a comprehensive comparative study of all common cleaning processes; such a study has yet to be completed. Experience gained from the research presented in this thesis prompts the recommendation that anyone undertaking AFM work take great care to plan, document, and report all surface preparation techniques such that the process and its results are reproducible.

When obtaining force curves with the AFM, there are several settings that must be adjusted in order to acquire a "good" force curve (see section 11.4.1 of the MultiMode SPM Instruction Manual, (2004)). A cautionary word: a force curve that looks acceptable in real time output (via the NanoScope software) is not necessarily the best that can be obtained. Data should be inspected using a graphing program such as Excel

that can display the force data with higher resolution before the determination is made that the settings used to obtain that force curve were the best possible. Care should then be taken to optimize the scan rate, ramp rate, and Z-limit, with the objective of resolving that portion of the force curve in which the researcher is most interested. In this study, the region from 0 nm separation to 50 or 60 nm separation was of most interest, rendering useless the majority or the instrument's 2500 nm vertical range and suggesting optimization efforts be focused on the 0- to 60-nm range.

The last topic deserving more attention is that of data analysis methodology. Manual conversion of deflection data into force curves is a very subjective process, particularly the definition of the distance of zero separation (Burnham et al., 1993; Senden, 2001) and the deflection of zero force. It is nonetheless the accepted method by which AFM data are converted to force curves (Ducker et al., 1992). Also accepted is the tenant that several sets of data must be averaged for the generation of one representative force curve. In some cases, small variations in the averaging technique can have a significant impact on the reported force curve. It is therefore critical that the techniques used in defining zero separation and zero force and in averaging raw data be well documented. Because of the time-intensive nature of the conversion process, it would be worthwhile for future research to include a systematic study on determining the optimal number of raw data sets and/or work to develop a reliable automated conversion process.

Appendix A: Atomic Force Microscopy Background

In reviewing this thesis, it will be useful for the reader to have an understanding of AFM, force-distance data obtained from AFM, a force curve as predicted by theoretical calculations and its AFM counterpart, and a typical force curve obtained from AFM measurements made in this study.

The Atomic Force Microscope, invented in 1986 by Binnig et al. (1986), is a Scanning Probe Microscope operated in force mode, employing a specialized probe (i.e., cantilever beam with an ultrasmall mass, characterized by spring constant k) to measure forces as small as 10^{-18} N. The basic operational premise is as follows: a laser spot shines on a reflective cantilever and as the tip of this cantilever interacts with a sample consisting of a substrate of interest, typically on the order of 1 cm × 1 cm in size, it will deflect and the reflected laser signal is captured by a photodiode detector (Figure A- 1:). In this system, the instrument attempts to keep the cantilever stationary and the movement of the substrate is carefully controlled in the vertical direction by a piezoelectric scanner.

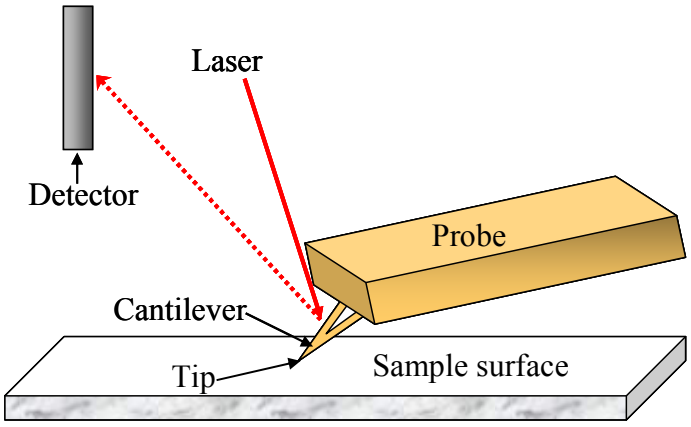

Figure A- 1: Cartoon showing basic operational premise of AFM.

With this system, the deflection of the cantilever is captured as a function of the vertical displacement of the scanner. Conversion of these AFM data, an example of which is shown in Figure A- 2, to force-distance data requires determination of the slope of the region of constant compliance, the average voltage in the region of zero force, and that the spring constant of the cantilever is known.

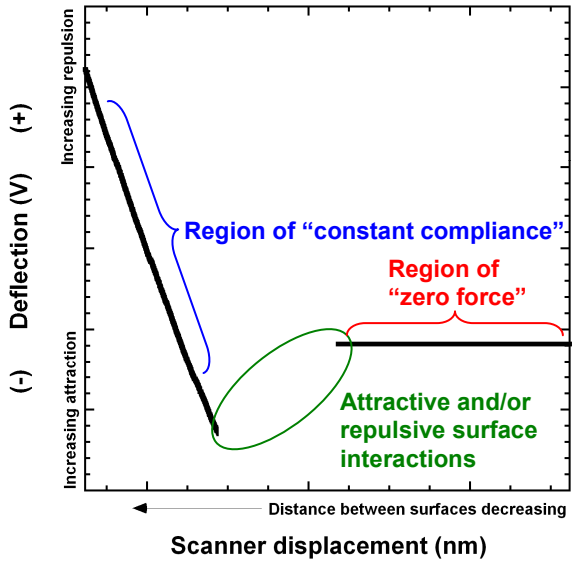

Figure A- 2: Schematic representation of AFM output for colloid-surface interaction.

Force as a function of the separation distance between a tip and a sample can also be estimated by the theoretical predictions of the Derjaguin-Landau-Verwey-Overbeek (DLVO) theory Figure A- 3a. The total interaction force (black line) is the sum of the repulsive electrostatic double-layer forces (green line) and the attractive van der Waals forces (red line). There are several important concepts illustrated in Figure A- 3a: 1) Repulsive forces are positive and attractive forces are negative; 2) At a large separation distance, no force is felt; 3) As the separation distance between the surfaces decreases, a

series of attractive (minima) and repulsive (maxima) regions can be encountered. Figure A- 3b gives a schematic representation of a deflection versus scanner displacement curve obtained from AFM measurements that would correspond to the types of interactions shown in Figure A- 3a.

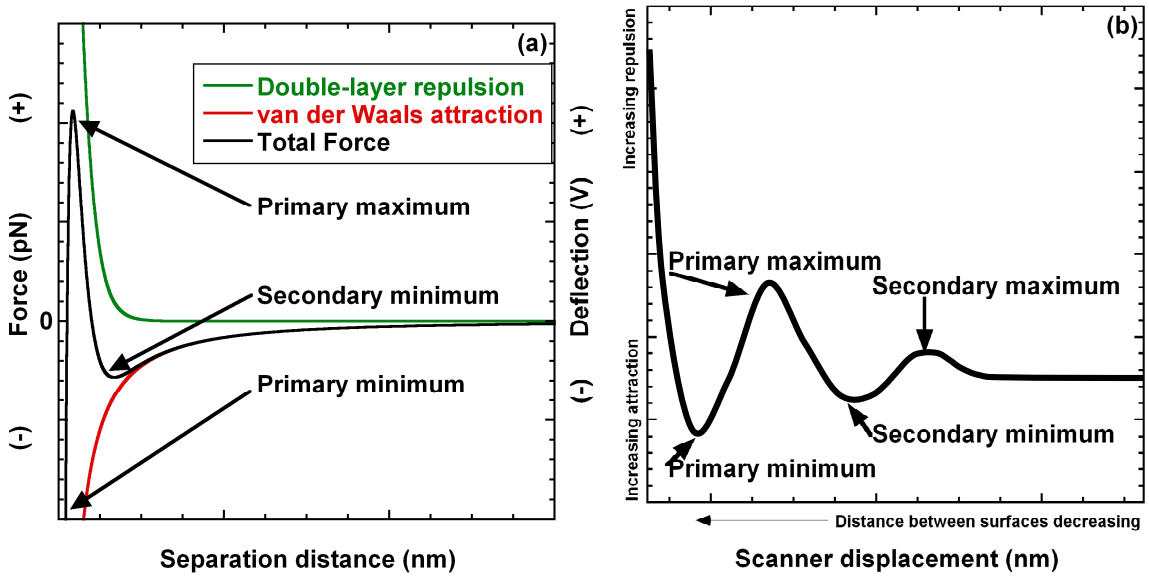

Figure A- 3: Schematic representation of force-distance curves from theoretical calculations (a) and AFM measurements (b). The theoretical curves are for two charged surfaces interacting across an electrolyte solution, after Israelachvili Fig.12.12 (Israelachvili, 1992).

The critical similarities between the theoretically-generated and AFM-measured curves are the region of zero force, the secondary minimum, and the primary maximum, all features which appear similar in both curves. At a different scale, the theoretical curves would also show a secondary maximum, as this feature must precede any minimum. The apparent differences between the curves are manifestations of the primary minimum and region of constant compliance. The theoretical force curve suggests the primary minimum approaches -∞, where the AFM measured curve shows the attractive primary minimum at a finite negative deflection, followed by the strong repulsion of the region of

constant compliance. Both curves do in fact exhibit the same features; however, for the theoretical curves, because the magnitude of the depth of the primary minimum is much greater than the height of the primary maximum, it is difficult to observe both on the same plot. The theoretical total force curve does in fact reach an inflection point at a very large negative value (i.e., the primary minimum) and, at a separation distance nearly equal to zero, approaches $+\infty$, which is equivalent to a strong repulsive force and the region of constant compliance observed via AFM.

Finally, it is important to note the critical differences between the deflection-scanner displacement curves shown in Figure A- 3b and the curves actually obtained from AFM measurements made in this study (Figure A- 4).

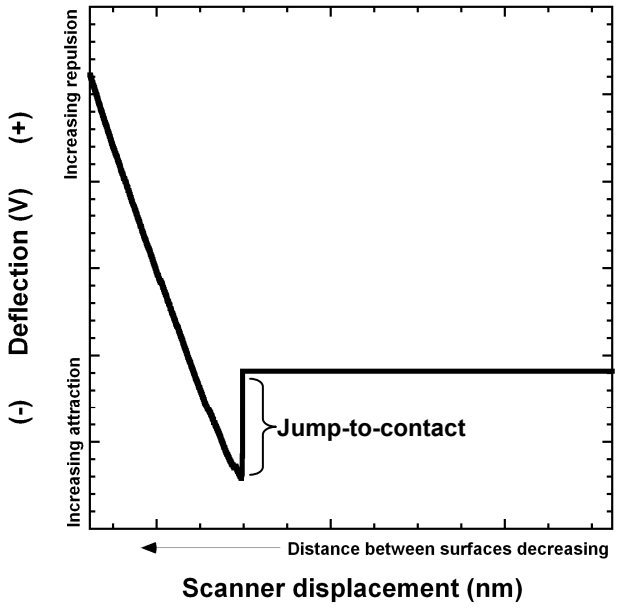

Figure A- 4: Schematic representation of typical AFM output for colloid-surface interaction measured in this study.

The regions of constant compliance and zero force were observed as expected; however, it is in the region where attractive and/or repulsive interactions should be measured (see

Figure A- 2) that the major discrepancy arose. Instead of observing a series of maxima and minima as the surfaces were brought together, zero-force was observed followed by a sharp decrease in voltage at the "jump-to-contact" point, immediately succeeded by the region of constant compliance. Jump-to-contact occurs when the force gradient between the tip and the sample exceeds the force gradient of the cantilever spring constant. Recalling the theoretically predicted force-distance curve (Figure A- 3b), the force at jump-to-contact is an indication that the primary force maximum has been overcome. Figure A- 2 through Figure A- 4 will provide useful reference information as force-distance curves are presented and discussed in the manuscript.

Appendix B: Averaging and Oscillation Removal

To ensure that the averaging technique was not imposing an unintended bias on the reported data, the two different methods by which data can be averaged were evaluated for the entire 4 Oct 2006 data set and for relevant portions of the 2 Oct 2006 and 6 Jan 2007 data sets. One method for averaging involves aligning and averaging the raw deflection versus sample displacement data before removing the oscillations; the other method requires that oscillations are removed from each of the 50 individual curves before they are aligned and averaged.

Results of this comparison are shown in Figure B- 1 for data collected on 4 Oct 2006. For all cases, the tip-sample separation distance is impacted to varying degrees. The determination of this value is somewhat arbitrary and can not be taken as absolute (Burnham et al., 1993; Senden, 2001); therefore, most attention is paid to the depth of the jump-to-contact point. Only for the 100 mM data does the averaging technique change the resulting force curve; depths of the jump-to-contact points differ by 50 pN. For 100 mM data collected on 2 Oct 2006 and 6 Jan 2007, both averaging techniques (not shown) yielded identical results (i.e., the depth of the jump-to-contact point was the same). In an effort to determine when the averaging technique would make a difference in the resulting force curves, the amplitude of the oscillations was correlated to the depth of the jump-to-contact portion of the deflection versus sample displacement curve. It was determined that only when the oscillation amplitude was greater than 10% of the depth of jump-to-contact did the method by which the data were averaged have an impact on the

final force versus tip-sample displacement curves. This relationship was used as a screening tool prior to analyzing raw AFM data.

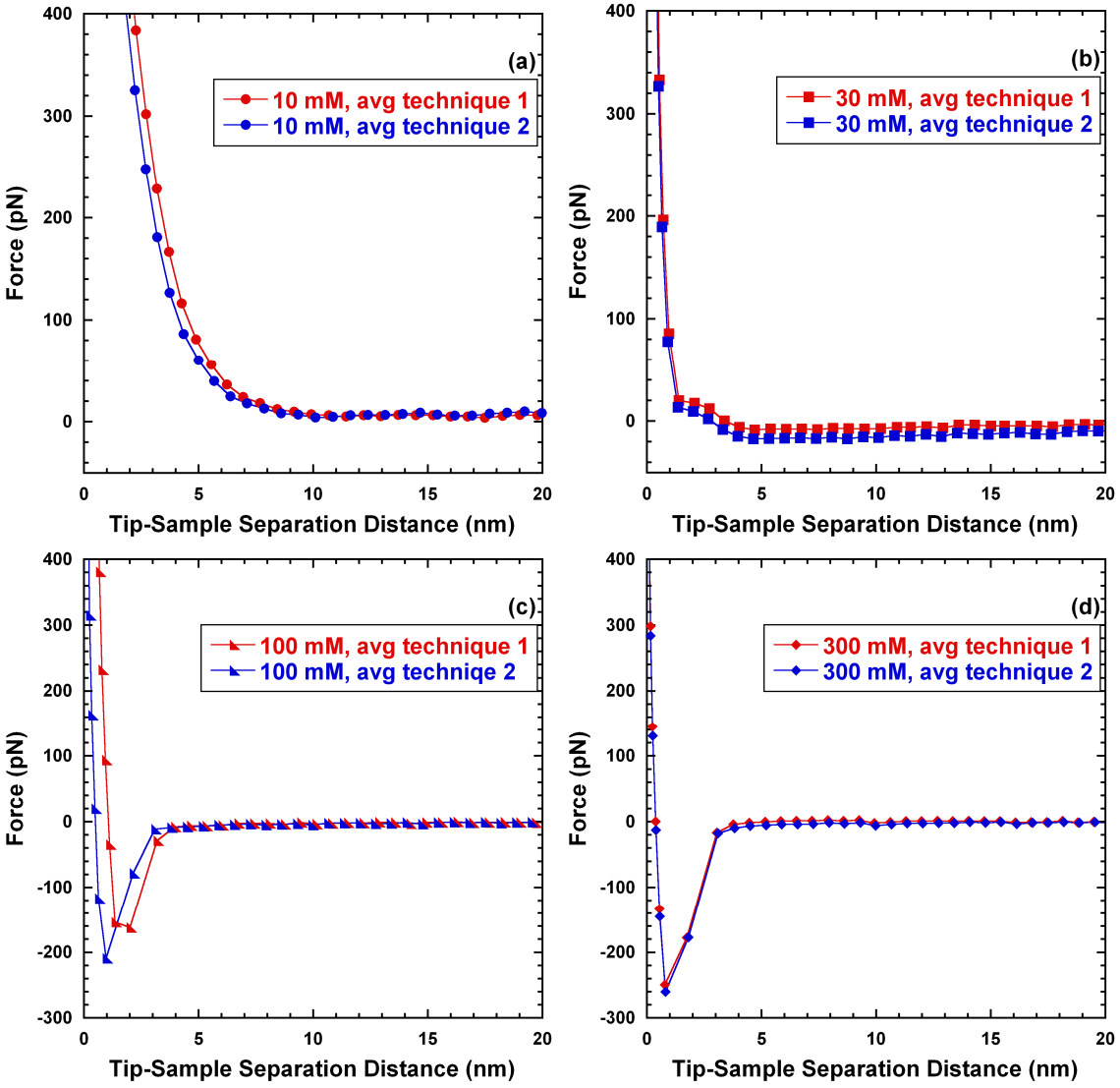

Figure B- 1: Force versus distance for data collected on 4 Oct 2006. (a) 10-mM KCl. (b) 30-mM KCl. (c) 100-mM KCl. (d) 300-mM KCl. Avg technique 1 (red points) give data where 50 raw AFM curves were averaged after removal of oscillations. Avg technique 2 (blue points) give data where 50 raw AFM curves were averaged before removal of oscillations.

Appendix C: AFM Measurements Not Reported in the Manuscript

Interaction forces were also measured for a 2-μm carboxyl-modified polystyrene latex microsphere interacting with a silica surface in KCl solutions of varying ionic strength. These measurements were performed with the intent of comparing interaction forces for the silica--KCl-microsphere system to those for the muscovite-KCl-microsphere system The silica surface was polished to a 1-μm finish (i.e., asperities on polished surface had a relief of less than 1 μm) by Sandia National Laboratories' Processing and Environmental Technology Laboratory. The experimental protocol for measuring interaction forces was similar to that employed for the muscovite-KCl-carboxyl-modified microsphere system, involving the following steps: (I) place prepared colloid probe (spring constant equal to 0.06 N/m) in fluid cell, (II) place silica on AFM sample stage, (III) mount the fluid cell in the AFM head, atop the silica surface with an o-ring between the two to provide a seal and prevent leakage, (IV) bring the silica surface and colloid probe into close contact (i.e., decrease separation distance between the two until the image of the cantilever and the image of the reflection of the cantilever are almost in the same optical plane), (V) optimize deflection signals, (VI) introduce 3 mL pure ethanol and allow to remain stagnant in fluid cell for 1.5 min and then flush with additional 2 mL (this served as the primary cleaning mechanism), (VII) flush system with 20 mL DI water, (VIII) introduce 10-mM KCl solution and allow system to equilibrate for 120 min turning laser and microscope light off to minimize heating of system, (IX) engage tip and obtain 50 force measurements, (X) disengage; repeat for 30-, 100- and 300-mM KCl solution. The major

differences between the force measurements conducted for the silica-KCl-carboxyl-modified microsphere system and the muscovite-KCl-carboxyl-modified microsphere system were (I) the system was not dissembled and reassembled between measurements days, meaning that the same silica surface and microsphere were used repeatedly, (II) the spring constant of the cantilever was 0.06 N/m as opposed to 0.32 N/m, (III) a strict cleaning protocol was not followed, (IV) electrolyte solutions were not prepared or stored in glass containers, (V) electrolyte solutions were introduced with disposable plastic syringes, as opposed to glass Gastight®, through silicone adapters, as opposed to Teflon, and (VI) deionized water was used, as opposed to 18 MΩ-cm water. The decision to alter much of the experiment protocol for the measurements made with the muscovite surface are worth noting and are as follows: (I) the muscovite surface replaced the silica surface because the process by which the muscovite surface is cleaned is much easier and less hazardous (i.e., cleaving the muscovite to expose a clean surface is preferred over Pirahna etching of the silica surface, which requires exposure of the silica surface to a 1:1 mixture of 18 M H_2SO_4 and 30% H_2O_2 in order to expose a fresh oxide layer), and the muscovite surface is molecularly smooth, removing the effects of topography heterogeneities, (II) a stiffer spring constant was chosen with the rational that this would reduce noise in the baseline data, (III) it was determined that minimization of system impurities was likely to facilitate reproducibility of results, hence 18 MΩ-cm water replaced deionized water, glass containers (that could be acid washed) replaced plastic containers for storage of KCl solutions, and all system components were carefully cleaned. Those components that could not be subjected to robust cleaning were

replaced with components that could be (e.g., silicone adapters replaced by Teflon adapters). The primary objective driving these modifications was the desire to generate reproducible results that could be reported with confidence. It is lack of confidence in results and that have kept the results that follow from the main manuscript.

The results from direct AFM observations for silica interacting with a carboxyl-modified polystyrene latex microsphere in KCl solutions of varying ionic strength are shown in Figure C- 1. Measurements were taken on two different days, the fluid cell-colloid probe- silica assembly was not dissembled and reassembled between measurements, though the system was thoroughly flushed with deionized water, and the same experimental protocol was employed on both days. Each plot gives force in pN versus tip-sample separation distance in nm. The results appear to be reproducible; however, analysis of these results was taken no further because determination of zero force involved arbitrarily picking a displacement range at a closer separation than is advisable and the trend as a function of ionic strength was inconsistent with theory. The displacement at which zero force was determined was smaller than usual (i.e., the surfaces were closer together), necessitated by the existence of an artifact that appeared to be a long-range attractive force. In terms of expected interactions as a function of ionic strength, the most repulsive forces should have been observed in 10 mM and repulsion should have decreased as ionic strength increased. AFM observations showed maximum repulsion in 300 mM, minimum repulsion in 100 mM, and an intermediate repulsion for 10- and 30-mM. This contradictory behavior was likely due to the fact that these surfaces were topographically heterogeneous, and is also attributable to the failure to employ

stringent surface and material preparation techniques. Future efforts should employ the strict cleaning procedures set forth in Cleaning Protocol of the manuscript and also include Pirahna etching of the silica surface.

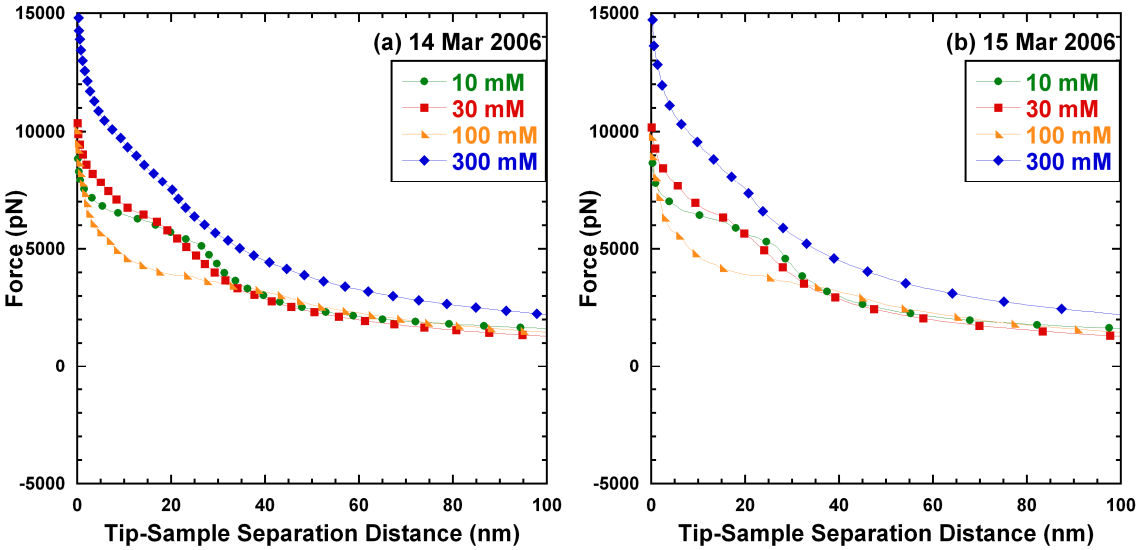

Figure C- 1: Force versus distance for AFM measurements of a silica surface interacting with a carboxyl-modified polystyrene latex microsphere in KCl solutions of varying ionic strength. Identical measurements were performed on two different days. (a) 14 Mar 2006. (b) 15 Mar 2006. Each curve is an average of 50 individual curves, analyzed as discussed in Atomic Force Microscopy Measurements of the manuscript. Oscillations due to optical interference were not observed for these data.

Appendix D: AFM Data

The 'AFM Data' CD provides all data corresponding to the measurements reported on in this thesis. A separate folder exists for each of the measurement days, using the naming convention 'day-month-year'. For measurements taken on 6 Jan 2007, an additional folder exists for the replicate measurements. In each main folder are two subfolders: 'Raw data' and 'Analyzed data'. 'Raw data' contains 50* text files: these are the ASCII files output directly from the AFM software, each providing scanner displacement (nm) and deflection (V). 'Analyzed data' contains an Excel file with numerical manipulations and the final reported data, using the naming convention 'day-month-year_colloid size_ionic strength range_mineral surface'. Some 'Analyzed data' folders may contain multiple Excel files with additional numerical manipulations. For example, for data collected in 100-mM KCl on 4 Oct 2006, multiple Excel files exist because 'avg technique 2' was used (see Appendix B: Averaging and Oscillation Removal), requiring many more calculations than 'avg technique 1'.All worksheets are organized and labeled in a consistent manner. Each individual worksheet uses descriptive headings, comments, and labeled plots to facilitate understanding of the content.

Questions regarding the data should be directed to Marissa D. Reno[1].

---

* In a very few cases, less than 50 force curves were obtained due to difficulties with the instrumentation. Explanatory notes are provided with these data sets.

[1] mdreno@sandia.gov, Sandia National Laboratories, Geohydrology Department, P.O. Box 5800, Albuquerque, NM 87185-0735

Thesis References

Veeco Instruments Inc., *MultiMode SPM Instruction Manual*, 2004.

Assemi, S., P. G. Hartley, P. J. Scales, and R. Beckett, 2004. Investigation of adsorbed humic substances using atomic force microscopy, *Colloid Surface A*, **248**, 17-23.

Bales, R. C., C. P. Gerba, G. H. Grondin, and S. L. Jensen, 1989. Bacteriophage transport in sandy soil and fractured tuff, *Appl. Environ. Microb.*, **55(8)**, 2061-2067.

Biggs, S., J. L. Burns, Y. Yao-de, G. J. Jameson, and P. Jenkins, 2000. Molecular Weight Dependence of the Depletion Interaction between Silica Surfaces in Solutions of Sodium Poly(styrene sulfonate), *Langmuir*, **16**, 9242-9248.

Binnig, G., C. F. Quate, and C. Gerber, 1986. Atomic Force MIcroscope, *Phys. Rev. Lett.*, **56**(9),

Bolster, C. H., A. L. Mills, G. M. Hornberger, and J. S. Herman, 1999. Spatial distribution of deposited bacteria following miscible displacement experiments in intact cores, *Water Resour. Res.*, **35**(6), 1797-1807.

Born, M., and E. Wolf, 1999, *Principles of optics*, Cambridge University Press, Cambridge, UK.

Bowen, W. R., and T. Doneva, 2000. Atomic Force Microscopy Studies of Membranes: Effect of Surface Roughness on Double-Layer Interactions and Particle Adhesion, *J. Colloid Interface Sci.*, **229**, 544-549.

Bowen, W. R., T. Doneva, and A. G. Stoton, 2002a. The use of atomic force microscopy to quantify membrane surface electrical properties, *Colloid Surface A*, **201**, 73-83.

Bowen, W. R., A. S. Fenton, R. W. Lovitt, and C. J. Wright, 2002b. The Measurement of *Bacillus mycoides* Spore Adhesion Using Atomic Force Microscopy, Simple Counting Methods, and a Spinning Disk Technique, *Biotechnol Bioeng*, **79**(2),

Bowen, W. R., N. Hilal, R. W. Lovitt, and C. J. Wright, 1998. A new technique for membrane characterisation: direct measurement of the force of adhesion of a single particle using an atomic force microscope, *J. Membrane Sci*, **139**, 269-274.

Bowen, W. R., N. Hilal, R. W. Lovitt, and C. J. Wright, 1999. An atomic force microscopy study of the adhesion of a silica sphere to a silica surface--effects of surface cleaning, *Colloid Surface A*, **157**, 117-125.

Bradford, S. A., J. Simunek, M. Bettahar, M. T. Van Genuchten, and S. R. Yates, 2003. Modeling Colloid Attachment, Straining, and Exclusion in Saturated Porous Media, *Environ. Sci. Technol.*, **37**, 2242-2250.

Bradford, S. A., S. R. Yates, M. Bettahar, and J. Simunek, 2002. Physical factors affecting the transport and fate of colloids in saturated porous media, *Water Resour. Res.*, **38**(12), **63-6**1-**63**-12.

Brant, J. A., and A. E. Childress, 2002. Membrane-Colloid Interactoins: Comparison of Extended DVLO Predictions with AFM Force Measurments, *Environ. Eng. Sci.*, **19**(6), 413-427.

Burnham, N. A., R. J. Colton, and H. M. Pollock, 1993. Interpretation of force curves in force microscopy, *Nanotechnology*, **4**, 64-80.

Butt, H.-J., 1991. Measuring electrostatic, van der Waals, and hydration forces in electrolyte solutions with an atomic force microscope, *Biophys. J.*, **60**, 1438-1444.

Butt, H.-J., J. Manfred, and W. A. Ducker, 1995. Measuring surface forces in aqueous electrolyte solution with the atomic force microscope, *Bioelectroch. Bioener* . **38**, 191-201.

Derjaguin, B. V., and L. Landau, 1941. *Acta Phys. Chim*, **14**(633-662),

Ducker, W. A., T. J. Senden, and R. M. Pashley, 1991. Direct measurement of colloidal forces using an atomic force microscope, *Nature*, **353**, 239-241.

Ducker, W. A., T. J. Senden, and R. M. Pashley, 1992. Measurment of Fores in Liquids Using a Force Microscope, *Langmuir*, **8**, 1831-1836.

Elimelech, M., and C. R. O'Melia, 1990. Kinetics of Deposition of Colloidal Particles in Porous Media, *Environ. Sci. Technol.*, **24**, 1528-1536.

Gebhardt, J. E., and D. W. Fuerstenau, 1983. Adsorption of polyacrylic acid at oxide/water interfaces, *Colloid Surface*, **7**(3), 221-231.

Gregory, J., 1981. Approximate Expressions for Retarded van der Waals Interaction, *J. Colloid Interface Sci.*, **83**(1), 138-145.

Grindrod, P., 1993. The impact of colloids on the migration and dispersal of radionuclides within fractured rock, *J. Contam. Hydrol.*, **13**, 167-191.

Grolimund, D., M. Elimelech, M. Borkovec, K. Barmettler, R. Kretzschmar, and H. Sticher, 1998. Transport of in Situ Mobilized Colloidal Particles in Packed Soil Columns, *Environ. Sci. Technol.*, **32**, 3562-3569.

Hahn, M. W., D. Abadzic, and C. R. O'Melia, 2004. Aquasols: On the Role of Secondary Minima, *Environ. Sci. Technol.*, **38**, 5915-5924.

Hahn, M. W., and C. R. O'Melia, 2004. Deposition and Reentrainment of Brownian Particles in Porous Media under Unfavorable Chemical Conditions: Some Concepts and Applications, *Environ. Sci. Technol.*, **38**, 210-220.

Harvey, R. W., L. H. George, R. L. Smith, and D. R. LeBlanc, 1989. Transport of Microspheres and Indigenous Bacteria through a Sandy Aquifer: Results of Natural- and Forced-Gradient Tracer Experiments, *Environ. Sci. Technol.*, **23**, 51-56.

Hogg, R., T. W. Healy, and D. W. Fuerstenau, 1965. Mutual Coagulation of Colloidal Dispersions, *T Faraday Soc.*, **66**, 1638-1651.

Israelachvili, J., 1992, *Intermolecular and Surface Forces*, Elsevier, London.

Israelachvili, J. N., and G. E. Adams, 1978. Measurement of forces between two mica surfaces in aqueous electrolyte solutions in the range 0–100 nm, *J. Chem. Soc., Faraday Trans. 1*, **74**, 975-1001.

James, S. C., and C. V. Chrysikopoulos, 2003. Effective velocity and effective dispersion coefficient for finite-sized particles flowing in a uniform fracture, *J. Colloid Interface Sci.*, **263**, 288-295.

Keller, A. A., S. Sirivithayapakorn, and C. V. Chrysikopoulos, 2004. Early breakthrough of colloids and bacteriophage MS2 in a water-saturated sand column, *Water Resour. Res.*, **40**,

Kersting, A. B., D. W. Efurd, D. L. Finnegan, D. J. Rokop, D. K. Smith, and J. L. Thompson, 1999. Migration of plutonium in ground water at the Nevada Test Site, *Nature*, **397**, 56-59.

Kuznar, Z., and M. Elimelech, 2007. Direct Microscopic Observation of Particle Deposition in Porous Media: Role of the Secondary Energy Minimum, *Colloid Surface A*, **294**, 156-162.

Lee, S., and M. Elimelech, 2006. Relating Organic Fouling of Reverse Osmosis Membranes to Intermolecular Adhesion Forces, *Environ. Sci. Technol.*, **40**, 980-987.

Lee, S., and M. Elimelech, 2007. Salt cleaning of Organic-Fouled Reverse Osmosis Membranes, *Water Res.*, **41**, 1134-1142.

Li, Q., and M. Elimelech, 2004. Organic Fouling and Chemical Cleaning of Nanofiltration Membranes: Measurements and Mechanisms, *Environ. Sci. Technol.*, **38**, 4683-4693.

Li, X., T. D. Scheibe, and W. P. Johnson, 2004. Apparent Decreases in Colloid Deposition Rate Coefficients with Distance of Transport under Unfavorable Deposition Conditions: A General Phenomenon, *Environ. Sci. Technol.*, **38**, 5616-5625.

Lower, S. K., C. J. Tadanier, and M. F. Hochellla, 2000. Measuring interfacial and adhesion forces between bacteria and mineral surfaces with bilogical force microscopy, *Geochimica et Cosmochimica Acta*, **64**(18), 3133-3139.

Lyklema, J., 1991, *Fundamentals of Interface and Colloid Science*, Academic Press, London.

Lyons, J. S., D. N. Furlong, and T. W. Healy, 1981. The Electrical Double-Layer Properties of the Mica (Muscovite)-Aqueous Electrolyte Interface, *Aust J. Chem*, **34**, 1177-1187.

McCarthy, J. F., and L. D. McKay, 2004. Colloid Transport in the Subsurface: Past, Present, and Future Challenges, *Vadose Zone J.*, **3**, 326-337.

McCarthy, J. F., and J. M. Zachara, 1989. Subsurface transport of contaminants, *Environ. Sci. Technol.*, **23**(5), 495-502.

McKay, L. D., R. W. Gillham, and J. A. Cherry, 1993. Field experiments in fractured clay till: 2. Solute and colloid transport, *Water Resour. Res.*, **20**, 1149-1162.

Piech, M., and J. Y. Walz, 2002. Direct measurement of depletion and structural forces in polydisperse, charged systems, *J. Colloid Interface Sci.*, **253**(1), 117-129.

Ralston, J., I. Larson, M. W. Rutland, A. A. Feiler, and M. Klein, 2005. Atomic Force Microscopy and Direct Surface Force Measurements, *Pure Appl. Chem.*, **77**(12), 2149-2170.

Redman, J. A., S. A. Walker, and M. Elimelech, 2004. Bacterial Adhesion and Transport in Porous Media: Role of the Secondary Energy Minimum, *Environ. Sci. Technol.*, **38**, 1777-1785.

Reimus, P. W., Transport of Synthetic Colloids through Single Saturated Fractures: A Literature Review, LA-12707-MS, Los Alamos National Laboratory, 1995.

Reno, M. D., Interaction Forces Measured by Atomic Force Microscopy for Muscovite and Carboxyl-Modified Microspheres as a Function of Ionic Strength, M.S. Thesis, New Mexico Institute of Mining and Technology, 2007.

Scales, P. J., F. Grieser, and T. W. Healy, 1990. Electrokinetics of the Muscovite Mica-Aqueous Solution Interface, *Langmuir*, **6**(3), 582-589.

Senden, T. J., 2001. Force microscopy and surface interactions, *Curr. Opin. Colloid In.*, **6**, 95-101.

Sirivithayapakorn, S., and A. Keller, 2003. Transport of colloids in saturated porous media: A pore scale observation of the size exclusion effect and colloidal acceleration, *Water Resour. Res.*, **39**(4),

Speilman, L. A., and S. K. Friedlander, 1974. Role of Electrical Double Layer in Particle Deposition by Convective Diffusion, *J. Colloid Interface Sci.*, **46**(1), 22-31.

Toikka, G., R. A. Hayes, and J. Ralston, 1996. Adhesion of Iron Oxide to Silica Studied by Atomic Force Microscopy, *J. Colloid Interface Sci.*, **180**, 329-338.

Tong, M., T. A. Camesano, and W. P. Johnson, 2005. Spatial Variation in Deposition Rate Coefficients of an Adhesion-Deficient Bacterial Strain in Quartz Sand, *Environ. Sci. Technol.*, **39**, 3679-3687.

Toran, L., and A. V. Palumbo, 1992. Colloid transport through fractured and unfractured laboratory sand columns, *J. Contam. Hydrol.*, **9**, 289-303.

Tufenkji, N., and M. Elimelech, 2004. Deviation from the Classical Colloid Filtration Theory in the Presence of Repulsive DLVO Interactions, *Langmuir*, **20**(25), 10818-10828.

Tufenkji, N., and M. Elimelech, 2005. Breakdown of Colloid Filtration Theory: Role of the Secondary Energy Minimum and Surface Charge Heterogeneities, *Langmuir*, **21**, 841-852.

Tufenkji, N., J. A. Redman, and M. Elimelech, 2003. Interpreting Deposition Patterns of Microbial Particles in Laboratory-Scale Column Experiments, *Environ. Sci. Technol.*, **37**, 616-623.

Veeramasuneni, S., M. R. Yalamanchili, and J. D. Miller, 1996. Measurement of Interaction Forces between Silica and α-Alumina by Atomic Force Microscopy, *J. Colloid Interface Sci.*, **184**, 594-600.

Verwey, E. K. W., and J. T. G. Overbeek, 1948, *Theory of Stability of Lyophobic Colloids*, Elsevier, Amsterdam.

Xu, L.-C., and B. E. Logan, 2005. Interaction Forces between Colloids and Protein-Coated Surfaces Measured Using an Atomic Force Microscope, *Environ. Sci. Technol.*, **39**, 3592-3600.

Yao, K.-M., M. T. Habibian, and C. R. O'Melia, 1971. Water and Waste Water Filtration: Concepts and Applications, *Environ. Sci. Technol.*, **5**(11), 1105-1112.